Structural Response to Reflected Detonations and Deflagration-to-Detonation Transition in H_2-N_2O Mixtures

Z. Liang, J. Karnesky and J. E. Shepherd
Graduate Aeronautical Laboratories
California Institute of Technology
Pasadena, CA 91125

Explosion Dynamics Laboratory Report FM2006.003

August 29, 2006

Prepared for Office of River Protection,
US Department of Energy, Richland, WA

Abstract

This report documents a series of 15 tests that were carried out to provide validation data for the hydrogen explosions in piping and ancillary vessels (HPAV) study being carried out for the Waste Treatment and Immobilization Plant (WTP) Project at the Hanford Site. The test vessel is a tube 1.25 m long and 127 mm inside diameter, closed at both ends and instrumented with pressure and strain gauges. Detonation waves were created by transition from deflagration to detonation when a flame was ignited at one end of the tube using a glow plug. The study used mixtures of hydrogen and nitrous oxide with hydrogen concentrations between 15 and 30%, an initial pressure of 1 bar and initial temperature of 22-25°C. In 12 tests, an array of tab obstacles was used to promote flame acceleration and in three tests, the tube had no obstacles.

Contents

List of Figures

List of Tables

1 Introduction

This report describes tests of the structural response of a pipe with a closed end to an internal loading due to detonation created by a deflagration-to-detonation transition (DDT) event. These tests were carried out to support the Hydrogen explosions in Piping and Ancillary Vessels (HPAV) study being carried for the Waste Treatment and Immobilization Plant (WTP) Project at the Hanford Site. The purpose of these tests is to provide data for the validation of computations of structural response to detonations of hydrogen-nitrous oxide mixtures inside pipes.

Two series of tests were performed with different mole fractions of H_2 and internal tube configurations. Test series A consists of three tests with 30% H_2 and no obstacles within the tube. This mixture and tube configuration were chosen in an effort to produce deflagration to detonation transition near the tube end. These tests are a follow on to an initial set of 50 preliminary tests that were used to estimate thresholds to DDT. Issues with the transducer calibration and gauge mounting (the transducer in the end wall was recessed, creating artifacts in the signal) were identified in the first series of tests and resolved for the tests that are reported here.

Test series B consists of twelve tests, four at 15% H_2, four at 17%, two at 20%, and two at 30% . For these tests, rectangular tabs, with a blockage ratio of 0.25, were mounted inside the tube to accelerate the flames and promote transition to detonation. Tests at 15% resulted in transition to detonation close to the far end of the tube (opposite to the ignition location), tests at 30% resulted in transition close to the ignition point. All of the mixtures tested had similar Chapman-Jouguet (CJ) pressures (Table 1) but the flame speeds (Pfahl and Shepherd, 1997, Pfahl et al., 2000, Kaneshige et al., 2000), detonation velocities, and cell sizes (Akbar et al., 1997, Kaneshige and Shepherd, 1997, Pfahl et al., 1998b,a) are a function of composition and initial pressure; this will influence the DDT behavior and should be considered when extrapolating this data to other conditions. The detonation cell width has a minimum value at 50% H_2 and increases with decreasing H_2 concentration or increasing air dilution. From the previous studies (Pfahl et al., 1998a), the detonation cell width dependence on hydrogen concentration at 100 kPa initial pressure and room temperature has been estimated and is shown in Table 1. The CJ properties were computed using a thermochemical equilibrium code (Reynolds, 1986) using an initial temperature of 300 K and an initial pressure of 100 kPa with a product species set of H, HNO, HO, HONO, H_2, H_2O, H_3N, N, NH, NH_2, NNH, NO, NO_2, N_2, N_2O, O, O_2.

All tests were carried out in a 127 mm (5 in) diameter and 1.25 m (49 in) long tube with a 12.7 mm (0.5 in) thick wall. The data consist of pressure and strain histories measured

Table 1: Estimated detonation properties for H_2-N_2O mixtures at 300 K and 100 kPa. λ - detonation cell width, U_{CJ} - CJ detonation velocity, P_{CJ} - CJ detonation pressure, c_{CJ} - CJ detonation product sound speed.

H_2 (vol %)	λ (mm)	U_{CJ} (m/s)	P_{CJ} (MPa)	c_{CJ} (m/s)
50	1.5	2394	2.52	1300
30	3.2	2092	2.60	1142
20	4.6	1959	2.57	1076
13	9.1	1869	2.52	1032

at select locations on the tube. The key results are summarized in this report with graphs and tables. The peak pressures and strains are compared to computed values that would be predicted on the basis of quasi-static structural loading. In addition to this report, the data are available as ascii files[1] to enable detailed analysis and comparison with the simulation studies.

[1] `http://www.galcit.caltech.edu/~liangz/Experiments-H2N2O/CaltechResearch-H2N2O.html`

2 Experimental Set-up

All experiments were conducted in a vessel constructed of 316L stainless steel tubing with 2-in thick welded flanges and bolted closures. Mounts for 8 pressure transducer ports were welded to the tube as shown in Fig. 1. The vessel has a length of 1.25 m (49 in) as measured between the inner surfaces of the flanges, a tube inner diameter of 127 mm (5 in), and the tube wall thickness was 12.7 mm (0.5 in). Dimensional drawings of the tube and internal configuration are shown in Figs. 8 and 9 of Appendix B. The period of oscillation for the fundamental hoop mode is 85 μs, corresponding to a frequency of 11.7 kHz. This is the characteristic frequency with which we expect to observe oscillations in the strain signals, see Beltman and Shepherd (2002), Shepherd (2006). The characteristic length over which bending relaxes is 23 mm. This is the distance (Shepherd, 2006) over which a localized load will be observed to influence the radial deformation of the tube. The tube wall is sufficiently thick and the initial pressure sufficiently low that all of the deformations were elastic in the present experiments. The peak hoop strain observed in the testing was less than 0.06%.

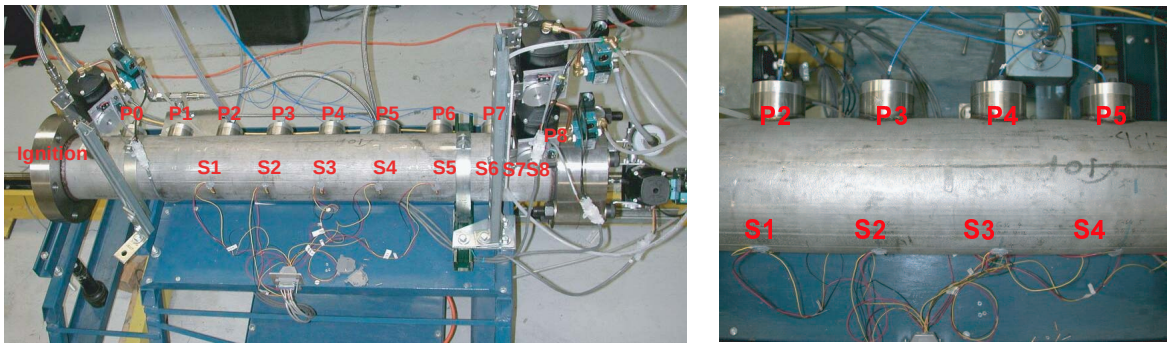

a) b)

Figure 1: Experimental setup. a) 9 Pressure transducer ports (P_0-P_8), and 8 strain gauges (S_1-S_8). Ignition flange is to the left. b) Top view: Pressure transducers P_2-P_6 and strain gauges S_1-S_5 are mounted opposite each other.

For test series B, the detonation tube had an obstacle insert, shown in Fig. 9. Rectangular tab obstacles (1 in wide, 1.375 in high and 0.25 in thick) are mounted on four 1/2-in threaded rods, equally spaced, with 5 tabs on each rod. The spacing of the obstacles is 127 mm (1.0 D) and the blockage ratio is 0.25, which is the ratio of projected area of the obstructions within the tube to the cross-sectional area. The four rods are attached to the ignition end flange closure.

Prior to filling, the tube is evacuated below 5 Pa. The tube is filled by the method of partial pressure with H_2 and N_2O, and the gas is circulated by a bellows pump for five minutes to ensure a homogeneous mixture. The filling lines are evacuated between switching

gases in order to minimize the filling error caused by residual gas. A sample checklist used for controlling the test procedure is shown in Appendix A

The static pressure was measured with a Heise digital pressure gauge (Model 901 A, accuracy 0.07%, pressure range 1-250 kPa). It was last calibrated on Feb. 24, 2004. An Omega type K unshielded thermocouple was installed on the right end flange, and read out with an Omega DP116-KC2 meter. The mixture was ignited by applying a voltage of 10 V (at a current of 9.5 A) to a glow plug (Bosch 0-250-202-051) which was mounted in the center of the left flange.

Pressure transducer ports (P_0-P_7) were welded onto the tube sidewall and spaced at a distance of 127 mm; see Fig 1a and locations in Table 3. A single pressure transducer port (P_8) was mounted on the end flange opposite the igniter. The pressure transducers were mounted in plugs that fit snugly within the ports, and the sensitive surface of the transducers was flush with the interior surface of the tube. Only pressure transducer ports P_1-P_8 were equipped with pressure transducers, and the remaining port P_0 was filled with a blank plug. Since the measured peak pressure varied over a large range depending on location, several different piezoelectric pressure transducer (PCB) models 113A24 and 113A23 were used; these have a dynamic range of 69 bar and 1034 bar, respectively. The gauge types and conversion factors are listed in Table 2. The PCB gauges were connected to a PCB Model 482A22 Signal Conditioner.

Table 2: Pressure transducer types, ranges, and calibration information.

Type	Serial Number	Conversion Factor mV/MPa	Port Number P_1-P_8	Date calibrated mm/dd/yy
113A24	SN 13908	724.8	P_1	10/22/2003
113A24	SN 13276	720.5	P_2	02/03/2003
113A24	SN 13278	728.8	P_3	02/03/2003
113A24	SN 13909	727.7	P_4	03/14/2006
113A24	SN 13277	700.4	P_5	03/14/2006
113A24	SN 14835	702.5	P_6	03/14/2006
113A24	SN 14771	732.4	P_7	03/14/2006
113A23	SN 14756	71.93	P_8	03/14/2006

Eight strain gauges (S_1-S_8) are mounted on the outer tube surface. The first five gauges S_1-S_5 are directly opposite the pressure transducer ports P_2-P_6, and the last three gauges S_6-S_8 are more closely spaced; see Fig 1b and locations in Table 3. The strain gauges are of type CEA-06-125UN-350 (Vishay Measurements Group, Micro-Measurements Division), have a uni-axial strain gauge pattern, and are oriented to measure the hoop strain of the

tube. The gauges are operated with an excitation voltage of 10 V in the quarter bridge mode using the built-in 350 Ω dummy gauges of the signal conditioning amplifiers (Type 2310A, Vishay Measurements Group, Micro-Measurements Division). An amplification factor of 500 for the strain gauge signals was used. The bridge circuits are balanced prior to the ignition event.

The pressure and strain histories were recorded with a 14-bit National Instruments (NI-PXI-6133 modules) data acquisition system simultaneously sampling all channels. A sampling frequency of 2 MHz and a total recording length of 30 ms were used in all tests. The data acquisition system was triggered by the rising edge of the first pressure transducer signal (P_1). The rise time of the transducers is on the order of 1 μs.

Table 3: Location of gauges.

Station	X (in)	X (mm)
Pressure		
IGNITION	0	0
P0	7	177.8
P1	12	304.8
P2	17	431.8
P3	22	558.8
P4	27	685.8
P5	32	812.8
P6	37	939.8
P7	42	1066.8
P8	49	1244.6
Strain		
S1	17	431.8
S2	22	558.8
S3	27	685.8
S4	32	812.8
S5	37	939.8
S6	41	1041.4
S7	43	1092.2
S8	45	1143

3 Experimental Results

Two test series, A and B, were carried out (see Table 4). Test A includes 3 repeat shots for 30% H_2. In Test B, the mole fraction of H_2 in the H_2-N_2O mixture was varied between values of 15%, 17%, 20% and 30% H_2 with between 2 and 4 repeat shots per case. A total of 15 experiments were carried out. A complete list of the experiments is given in Table 5 and the pressure and strain histories are given in Appendix C.

Table 4: Summary of test series.

Series	Mole fraction of H_2	T_0 (°C)	P_0 (bar)	tube insert	total tests
A	30%	21-25	1.0	no obstacles	3
B	15%- 30%	21-25	1.0	tab obstacles	12

The pressure and strain signals were analyzed using computed values of the peak pressure for idealized combustion processes. The values for CJ pressure (P_{CJ}), reflected CJ pressure (P_{CJref}) and constant volume explosion pressure (P_{CV}) are calculated using a chemical equilibrium program (Reynolds, 1986) as described in the Introduction. As mentioned previously, the CJ detonation pressure is similar for all of these mixtures and is approximately 2.5-2.6 MPa, with reflected detonation pressure of approximately 6.4 MPa. The detonation velocity decreases with decreasing hydrogen concentration (see Table 1) but the increasing initial mixture density compensates for that, resulting in the weak dependence of detonation pressure on composition.

The experimental peaks P_{max} and ϵ_{max} are the maximum measured pressure on the transducers located on the side of the tube (P_1-P_7) and maximum strain recorded on the strain gauges (S_1-S_8), respectively. $P_{8,max}$ is the measured maximum pressure on P_8 and is taken to be representative of the peak pressure on the flange at the end opposite the ignition point. The estimated location of transition to detonation is given in terms of the pressure transducer location in the "DDT" column and location of the peak strain is given in the "S_{max}" column. The peak pressure on the side gauges is usually found close to the estimated location of DDT.

The location of DDT onset was determined by examining the pressure traces for the characteristic signatures of DDT. Near the DDT location, the pressure peak will have a sharp front and a value several times higher than the CJ pressure P_{CJ}. For transducers between the ignition and DDT location, a gradual rise in pressure or sometimes weak shock waves are observed prior to the DDT event. The DDT event produces strong shock waves in the burned gas that can be observed as sharp jumps in the pressure signals that propagate

away from the DDT location and can be observed in transducers adjacent to the DDT event at later times. If the DDT location is sufficiently far from the end of the tube, a propagating detonation will be produced and can be observed on transducers downstream of the DDT location as a sharp front (rise time less than 1-5 μs) with a pressure comparable to the CJ value and speed comparable to the CJ speed. DDT events and propagating detonations also produce structural oscillations, including flexural waves as discussed in Beltman and Shepherd (2002), Shepherd (2006), that create very distinctive high frequency signals in the strain gauges. The onset of these signals in the strain gauges can be used to help confirm the location of DDT. The results for all tests are summarized in Table 5

Table 5: Summary of all tests. Initial conditions were 1 bar and 22-25°C in all cases.

shot	P_{CV} (MPa)	P_{CJ} (MPa)	P_{CJref} (MPa)	$P_{8,max}$ (MPa)	P_{max} (MPa)	DDT	ϵ_{max} (μstrain)	S_{max}
Test series A for 30% H_2, no obstacles.								
67	1.32	2.60	6.46	16.0	5.86	P7	387	S8
68	1.32	2.60	6.46	16.8	13.6	P7	465	S8
69	1.32	2.60	6.46	13.8	9.76	P7	364	S8
Test series B for 15% H_2, with obstacles.								
62	1.29	2.54	6.27	25.1	7.28	P7	554	S8
64	1.29	2.54	6.27	17.6	–	P7	325	S8
66	1.29	2.54	6.27	24.3	6.85	P7	351	S8
72	1.29	2.54	6.27	23.1	6.99	P7-P6	570	S8
Test series B for 17% H_2, with obstacles.								
56	1.30	2.55	6.32	30.5	6.35	P4	352	S6
59	1.30	2.55	6.32	30.5	14.3	P5	297	S6
70	1.30	2.55	6.32	41.0	5.11	P4-P5	347	S8
71	1.30	2.55	6.32	20.3	13.8	P5	327	S6
Test series B for 20% H_2, with obstacles.								
60	1.31	2.57	6.37	24.7	9.89	P3	258	S6
61	1.31	2.57	6.37	23.4	10.9	P4	238	S5
Test series B for 30% H_2, with obstacles.								
57	1.32	2.60	6.46	12.9	6.82	P1	253	S6
58	1.32	2.60	6.46	13.3	7.85	P1	243	S6

3.1 Test series A: without obstacles

Tests 67, 68, and 69 were carried out at an H_2 concentration of 30% without any obstacles in the tube. These tests resulted in transition to detonation in the portion of the tube between P_7 and the end wall (P_8). There was some variability in the results which is typical for DDT

tests. The pressure traces and strain histories of shot 68 are shown in Fig. 2. The onset of detonation occurred near the last pressure transducer P_7 after the reflection of the shock wave generated by the accelerating flame. The shock is visible on P_8 as the step in pressure at about 1.6 ms, about 0.2 ms ahead of the main wave. The average (over the tests in this series) values for normalized pressures and the dynamic load factors for this series are given in Table 6. These tests resulted in the largest values of impulse at the end wall, see Table 11 but the peak pressures on the end wall were lower than all those in series B tests except with 30% H_2.

Table 6: Test series A characterization. See the discussion in Section 3.4 below for the definition of the dynamic load factors Φ.

P_{max}/P_{CJ}	Φ_{exp}	$P_{8,max}/P_{CJref}$	Φ_{CJref}
3.75	1.61	2.40	2.34

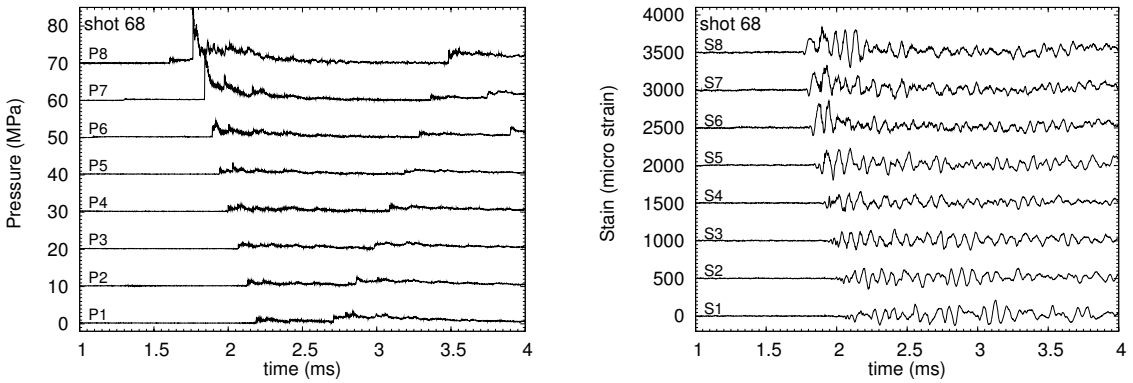

Figure 2: (a) Pressure traces and (b) strain histories of shot 68 for test series A, 30% H_2 without obstacles.

3.2 Test series B: with obstacles

3.2.1 15% H_2

Shots 62-66 were conducted with 15% H_2 and obstacles. Shot 64 had a loose cable on one transducer, otherwise the data are free from artifacts. In these tests, the location of DDT appeared to be close to P_7 although there was some significant variability. Data from two representative traces, shots 66 and 62, are shown in Figs. 3 and 4. Like the shots in test series A, onset of detonation is near the last pressure transducer P_7 and occurs after the reflection of a series of shock waves generated by the high speed deflagration that preceeded

the detonation. The peak pressures on the end wall were similar for the two tests but the peak strains were quite different, 554 μstrain for shot 62 and 351 μstrain for shot 62. This is because the peak strain occurs close to the end and is the result of interference between direct and reflected flexural waves. The flange is a large stiff mass that effectively acts as a "built-in" boundary condition for the mechanical motion of the tube. The average (over the tests in this series) values for normalized pressures and the dynamic load factors Φ (see discussions in section 3.4) for this series are given in Table 7. The peak pressure on the end wall is higher on average for these tests than in test series A but the impulse is lower, presumably due to the obstacles in the tube removing some of the momentum from the flow behind the wave. The highest peak strains, and therefore the largest values of Φ_{CJref}, occurred in these tests.

Table 7: Test series B - 15% H_2 characterization.

P_{max}/P_{CJ}	Φ_{exp}	$P_{8,max}/P_{CJref}$	Φ_{CJref}
2.77	2.45	3.59	2.53

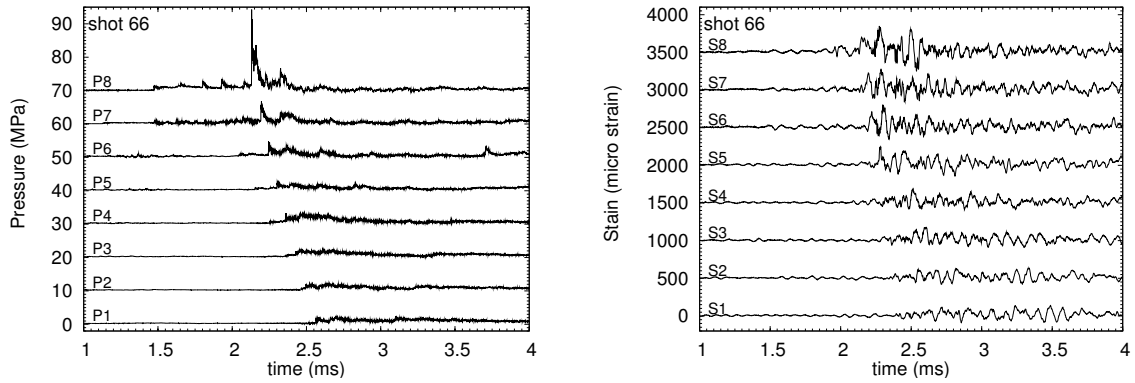

Figure 3: (a) Pressure traces and (b) strain histories of shot 66 for 15% H_2 at P_0=1 bar with obstacles.

3.2.2 17% H_2

Shots 56, 59, 70 and 71 were conducted with 17% H_2 and obstacles in the tube. Transition to detonation occurred close to P_4 or P_5 in these tests. The pressure traces and strain histories of shot 56 are shown in Fig. 5. The onset of detonation occurred earlier than the 15% H_2 case and no precursor waves are visible on the end wall pressure transducer. The average (over the tests in this series) values for normalized pressures and the dynamic load factors

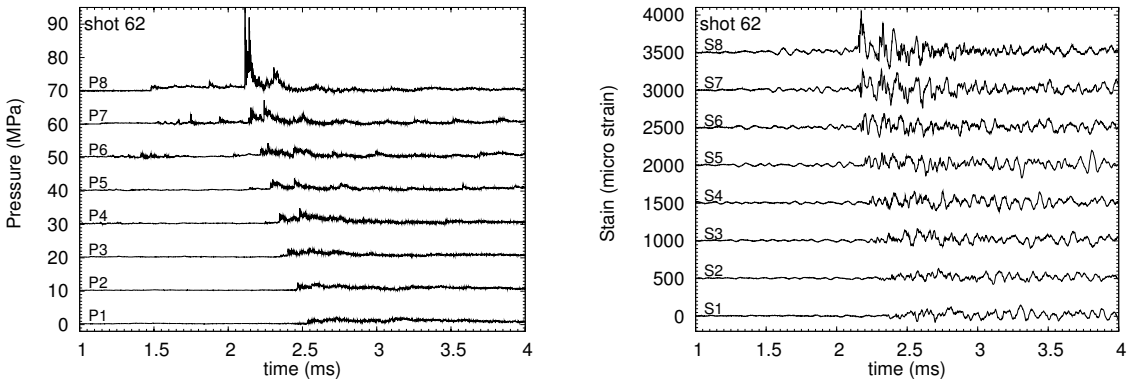

a) b)

Figure 4: (a) Pressure traces and (b) strain histories of shot 62 for 15% H_2 with obstacles.

for this series are given in Table 8. For all of these tests, a high-amplitude, short-duration pressure pulse is observed on P_8. These appear to be physical and are not artifacts. We speculate that these pulses are associated with the localized nature of the DDT process and may occur due to oblique shock or detonation wave reflection from the end wall. Although the peak pressure in these spikes can be as high as 30-40 MPa, the duration is so short that only a small increment in the impulse and deformation will be produced by these pulses. The dynamic load factor based on the computed reflected pressure is 1.84, consistent with an average loading pressure that is closer to 6 MPa, similar to that observed in the traces.

Table 8: Test series B - 17% H_2 characterization.

P_{max}/P_{CJ}	Φ_{exp}	$P_{8,max}/P_{CJref}$	Φ_{CJref}
3.87	1.48	4.84	1.84

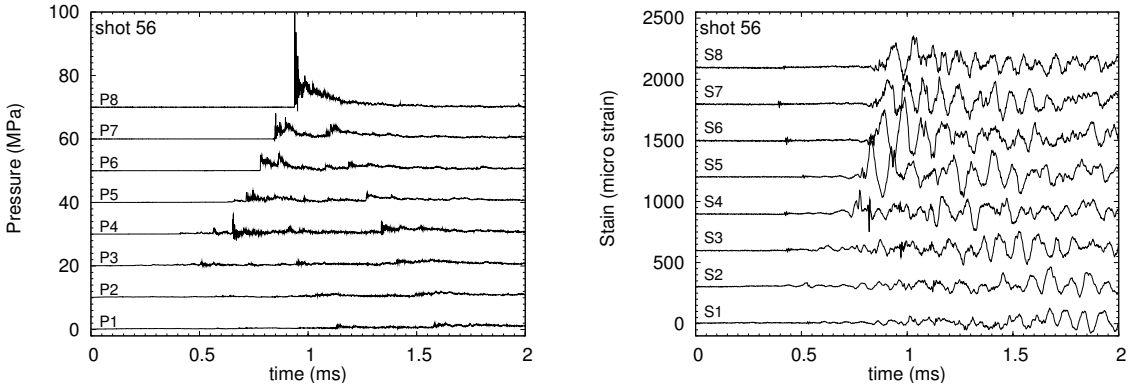

a) b)

Figure 5: (a) Pressure traces and (b) strain histories of shot 56 for 17% H_2 with obstacles.

3.2.3 20% H_2

Shots 60 and 61 were conducted with 20% H_2 with obstacles. In these tests, DDT occurred close to P_3 or P_4. The pressure traces and strain histories of shot 60 are shown in Fig. 6. The onset of detonation shifts farther from the reflecting end flange, close to P_3 or P_4. The average (over the tests in this series) values for normalized pressures and the dynamic load factors for this series are given in Table 9. The results are quite similar to the case with 17% H_2.

Table 9: Test series B - 20% H_2 characterization.

P_{max}/P_{CJ}	Φ_{exp}	$P_{8,max}/P_{CJref}$	Φ_{CJref}
4.05	0.84	3.78	1.37

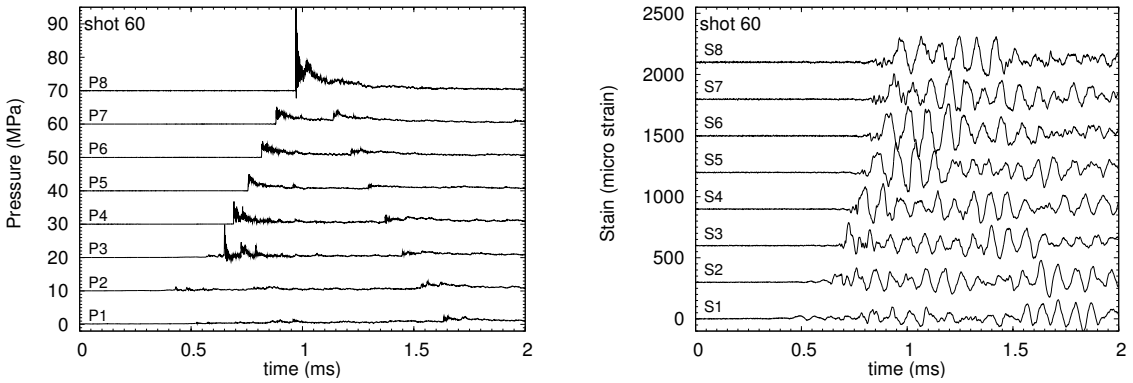

a) b)

Figure 6: (a) Pressure traces and (b) strain histories of shot 60 for 20 % H_2 with obstacles.

3.2.4 30% H_2

Shots 57 and 58 were conducted with 30% H_2 and obstacles in the tube. These tests simulated prompt initiation of the detonation since DDT occurred shortly after ignition. The pressure traces and strain histories of shot 57 are shown in Fig. 7. The onset of detonation occurred before P_1, the resulting propagating detonation wave and associated flexural wave can be seen in Fig. 7. The average (over the tests in this series) values for normalized pressures and the dynamic load factors for this series are given in Table 10. The peak pressures on the side and end wall are lower than in the other tests but at least twice the ideal values. The peaks are probably due to the secondary shock waves created when the propagating detonation reflects from the obstacles. Theses cases also had the smallest impulses of all the tests.

All pressure and strain gauge traces for shots 56-72 are shown in Appendix C.

Table 10: Test series B - 30% H_2 characterization.

P_{max}/P_{CJ}	Φ_{exp}	$P_{8,max}/P_{CJref}$	Φ_{CJref}
2.82	1.20	2.03	1.35

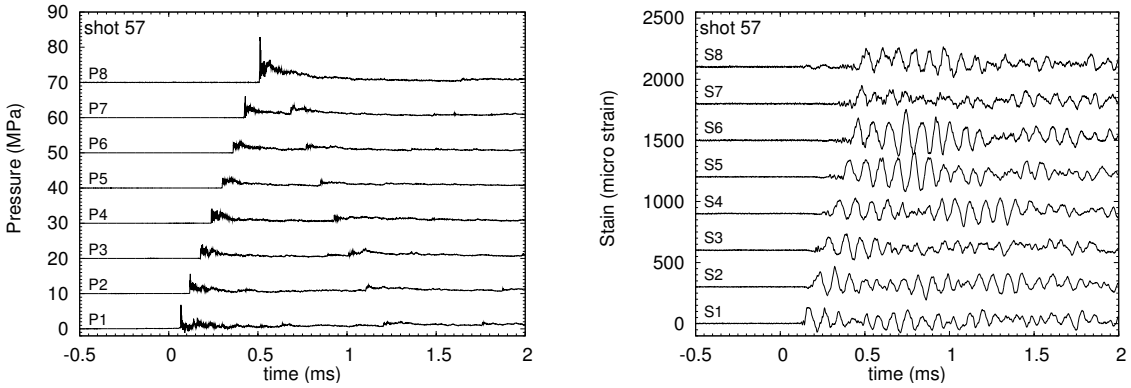

a) b)

Figure 7: (a) Pressure traces and (b) strain histories of shot 57 for 30% H_2 with obstacles.

3.3 Impulse of reflected pressure waves

One of the methods used to characterize the pressure-time histories is to compute the impulse or area under the pressure-time curves. The signals from the pressure transducer P_8 located on the end wall have been analyzed and the impulses (see table 11 computed by numerically integrating (using the trapezoidal rule) the pressure signal over a time interval selected individually so that the start corresponds to the detonation front arrival t_1 and the end of the integration period t_2 is prior to the arrival of the first reflected shock wave.

$$I_8 = \int_{t_1}^{t_2} P_8(t)dt \tag{1}$$

The minimum values of the impulse (1.57 kPa·s) are recorded for the nearly ideal case of detonations started early in the tube.

3.4 Pressure ratios and dynamic load factors

The peak pressures can be compared with the ideal values, P_{CJ} for propagating waves (P_1-P_7), and P_{CJref} for the end wall pressure signal P_8. Values higher than one for the ratio of the measured to the ideal value are a measure of the localized loading generated by the DDT process. Some caution in interpreting these values is in order because numbers larger than one are frequently observed due to the oscillations in the speed of the detonation front

Table 11: Impulse computed from pressure P_8 measured on the reflecting end flange.

shot	I_8 (kPa·s)	time period (t_1-t_2) (ms)
67	2.23	1.58-2.70
68	2.28	1.58-2.60
69	2.43	1.58-2.75
62	1.90	1.40-2.43
64	2.07	1.40-2.34
66	1.92	1.40-2.43
72	2.15	1.40-2.43
56	1.57	0.90-2.00
59	1.70	0.85-2.00
70	1.84	1.25-1.65
71	1.98	0.85-2.00
60	1.72	0.95-2.00
61	1.73	0.90-2.00
57	1.61	0.49-1.50
58	1.66	0.45-1.50

associated with detonation cellular structure (Shepherd, 2006). In some cases, particularly the 15 and 17% H_2 series, the pressure pulses associated with the peak values are extremely short in duration and therefore the contribution to the deformation is not in proportion to the maximum pressure but rather the impulse. The increment in deformation resulting from the impulses of these sharp pressure spikes is a small contribution to the overall deformation which is reflected in the measured peak strains.

The peak value of the strain signals can be analyzed by finding the dynamic load factor (DLF) Φ, which is defined as the ratio of the measured peak strain to the peak strain expected in the case of quasi-static loading[2]

$$\Phi = \frac{\epsilon_{max}}{\frac{\Delta P R}{E h}} \tag{2}$$

where $E = 193$ GPa, $R = 69.5$ mm (mean of inner and outer radius), $h = 12.7$ mm. Table 12 summaries the dynamic load factors computed with Eqn. 2. For Φ_{exp}, $\Delta P = P_{max}$ - P_a, with P_{max} obtained from column 6 in Table 5. These peak pressures are only for the gages P1-P7 mounted on the side of the tube, the location of the observed peak pressure is in column 7 of Table 5. For Φ_{CJref}, $\Delta P = P_{CJref}$ - P_a, where P_{CJref} is the ideal value for the peak

[2]This expression is based on simple membrane analysis. Most sophisticated solutions using the theory of elasticity include corrections for the Poisson effect and any longitudinal strain or stress that is induced by the boundary conditions at the tube ends.

pressure behind a reflected detonation, about 6.3 to 6.5 MPa for the present study (column 4 of Table 5).

The peak pressure in Eq. 2 can be based on either the measured peak value in the experiment or one of the computed values. Using the experimental pressure allows a rough[3] evaluation of what type of loading (impulsive, sudden or mixed) is taking place; using one of the computed values allows a comparison with assumed values used as part of the HPAV study. For an ideal single-degree of freedom structure and a simple pressure-time history with a single jump followed by a monotonic decay, values of Φ close to two are associated with the limit of "sudden loading" in which the pressure jumps to a high value and does not significantly decay on the time scale of the tube radial oscillation periods. In this regime, the peak elastic deformation is proportional to the peak pressure. As the decay time of the pressure after the jump becomes shorter, the DLF becomes less than two, decreasing as the decay time decreases. In the limit of very short pressure pulses, the loading is in the impulsive regime and the peak elastic deformation is proportional to the impulse. Between these two extremes, in the mixed regime, the peak elastic deformation will depend on both the impulse and peak pressure.

The values for the dynamic load factors in Table 12 range between 0.73 and 3.2. The values based on the experimental peak pressures are less than the values based on the computed ideal detonation reflection pressure. This is consistent with the very short duration of the measured pressure spikes associated with the highest pressures. If the pipe could be treated as a single degree of freedom structural system and the reference pressure rise (denominator in Eq. 2) bounded the applied load, then we would only expect values of the dynamic load factor less than two. However, values greater than two are observed in four (Φ_{exp}) or five (Φ_{CJref}) of the cases examined. There are several reasons why this may occur. In the case of the values based on the experimental pressures, the pressure and strain measurements are not completely consistent since the strain gauges close to the end wall are not exactly located at the same axial distance as the pressure transducers. For example, in test series A and B, the maximum strain was observed on S_8, which is 4 in away from the reflecting end flange but the peak pressure was observed on P7, which is 7 in away from the end flange. In case of values based on the reflected CJ detonation pressures, the effective applied pressure may be higher than this value due to pre-compression of the gas closest to the end flange.

In general, DDT is a localized event and the point measurements of pressure and strain do not represent either average or bounding values. The DDT event is unlikely to occur on the tube axis so that the pressure measured on one side of the tube will not be consistent with

[3]The observed pressure-time histories are sufficiently complex that characterization of the loading regime should be approached very cautiously.

the strain measured on the opposite side of the tube. Finally, from the strain signals, we can observe that the reflection and interference of flexural waves near tube flanges is important in determining the peak strain. These effects are due to having a extended (multiple degree of freedom) structure and traveling loads, a significantly more complex situation than a single degree of freedom model.

All of the factors mentioned above contribute to dynamic load factors greater than 2 being observed in some tests. When these considerations are combined with the inherent statistical fluctuations in the DDT process, we can also understand why the results (Table 12) for peak pressure and strain exhibit shot-to-shot variations for nominally identical initial conditions and configuration. The shot-to-shot variation in the dynamic load factor is largest for the cases with DDT close to the end flange. When the computed reflected detonation pressure is used to evaluate the dynamic load factor, a maximum value of 3.2 is found. The shot-to-shot variation decreases dramatically and the dynamic load factor is smaller when the DDT onset point moves upstream toward the ignition flange. This takes place as the hydrogen concentration is increased from 15% to 30%.

Table 12: Pressure ratio and dynamic load factors.

Shot	P_{max}/P_{CJ}	Φ_{exp}	$P_{8,max}/P_{CJref}$	Φ_{CJref}
Series A - 30% H_2, no obstacles				
67	2.25	2.32	2.48	2.11
68	5.23	1.20	2.60	2.76
69	3.75	1.31	2.14	2.16
Series B - 15% H_2, tab obstacles				
62	2.87	2.68	4.01	3.11
64	–	–	2.81	1.82
66	2.70	1.80	3.87	1.97
72	2.76	2.87	3.68	3.20
Series B - 17% H_2, tab obstacles				
56	2.49	1.95	4.82	1.96
59	5.59	0.73	4.82	1.66
70	2.00	2.39	6.49	1.93
71	5.39	0.84	3.21	1.82
Series B - 20% H_2, obstacles				
60	3.85	0.92	3.88	1.43
61	4.25	0.77	3.67	1.32
Series B - 30% H_2, obstacles				
57	2.62	1.31	2.00	1.38
58	3.02	1.09	2.06	1.32

4 Summary

The 15 tests carried out in this test program provide a range of structural loading associated with deflagration to detonation transition. The pressure and strain measurements can be used for the validation of simulations of fluid dynamics and structural response of tubes with a closed end. These cases are particularly relevant to the HPAV study for the WTP since the tests have been carried out with H_2-N_2O mixtures, in particular 30% H_2 which is considered to be a bounding case from the viewpoint of pressure loads.

There are two cases that are suitable for examining the situation of deflagration to detonation close to an end flange. For the tube set-up without obstacles, series A, the onset of detonation is close to the reflecting flange and occurs within the region influenced by precursor compression waves. For the tube set-up with obstacles, series B, the DDT run-up location shifts from the reflecting end flange to the ignition flange with increasing mole fraction of H_2. DDT occurs closest to the reflecting end for 15% H_2.

The two Series B cases of 17% and 20% H_2 have DDT events in the middle of the tube and are useful for examining that situation. The final case of 30% in series B is an approximation to promptly initiated detonation, with DDT taking place close to the ignition flange.

The maximum dynamic load factors, based on the strains measured near the end flange and the computed maximum pressure behind a reflected Chapman-Jouguet detonation, are on the order of 3.2 for cases that involve DDT near the tube end flange. The actual pressure loading has a complex spatial and temporal history with high amplitude, short duration pulses (spikes) superimposed on a waveform that consists of a jump (leading shock) followed by a gradual decay. The peak amplitude of the short duration pulses can be as high at 5.6 times the CJ pressure on the side of the tube and 6.5 times the pressure behind a reflected CJ detonation at the end wall. Although the strain signals show the oscillatory character observed in previous experiments with propagating detonations, sharp features associated with the DDT event and interference of reflected and incident flexural waves can also be observed.

For the purposes of safety assessments, we suggest that model pressure signals should be based on reproducing the observed peak strain values rather than the details of the pressure waves. If a simple pressure wave profile consisting of a square pulse followed by an exponential decay is used to model the load, the amplitude of the square pulse will have to be adjusted to yield the appropriate levels of peak strain. Depending on the duration of the initial pulse and the contribution of the exponential tail, observed deformations can be reproduced with peak pressures that are larger than the reflected CJ values but less than the peak values observed in the experiments.

Acknowledgments

This report was prepared for the Office of River Protection, US DOE and Lew Miller was the contract monitor.

Bibliography

R. Akbar, M. Kaneshige, E. Schultz, and J.E. Shepherd. Detonations in H_2-N_2O-CH_4-NH_3-O_2-N_2 mixtures. Technical Report FM97-3, GALCIT, July 1997. 6

W.M. Beltman and J.E. Shepherd. Linear elastic response of tubes to internal detonation loading. *Journal of Sound and Vibration*, 252(4):617–655, 2002. 8, 12

M. Kaneshige and J.E. Shepherd. Detonation database. Technical Report FM97-8, GALCIT, July 1997. See also the electronic hypertext version at http://www.galcit.caltech.edu/detn_db/html/. 6

M.J. Kaneshige, E. Schultz, U.J. Pfahl, J.E. Shepherd, and R. Akbar. Detonations in mixtures containing nitrous oxide. In G. Ball, R. Hillier, and G. Roberts, editors, *Proceedings of the 22nd International Symposium on Shock Waves*, volume 1, pages 251–256, 2000. 6

U. Pfahl, E. Schultz, and J.E. Shepherd. Detonation cell width measurements for H_2-N_2O-O_2-CH_4-NH_3 mixtures. Technical Report FM98-5, GALCIT, April 1998a. 6

U. Pfahl and J.E. Shepherd. Flammability, ignition energy and flame speeds in NH_3-H_2-CH_4-N_2O-O_2-N_2 mixtures. Technical Report FM97-4R1, GALCIT, July 1997. 6

U. Pfahl, J.E. Shepherd, and C. Unal. Combustion within porous waste. Technical Report FM97-18, GALCIT, February 1998b. Explosion Dynamics Laboratory Report to Los Alamos National Laboratory. 6

U.J. Pfahl, M.C. Ross, J.E. Shepherd, K.O. Pasamehmetoglu, and C. Ural. Flammability limits, ignition energy, and flame speeds in H_2-N_2O-CH_4-NH_3-O_2-N_2 mixtures. *Combustion and Flame*, 123:440, 2000. 6

W.C. Reynolds. The element potential method for chemical equilibrium analysis: implementation in the interactive program STANJAN. Technical report, Mechanical Engineering Department, Stanford University, 1986. 6, 11

J. E. Shepherd. Structural response of piping to internal gas detonation. In *ASME Pressure Vessels and Piping Conference*. ASME, 2006. PVP2006-ICPVT11-93670, to be presented July 23-27 2006 Vancouver BC Canada. 8, 12, 18

A Check list

```
 ####################  THICK TUBE setup ############################
 SHOTNUMBER 56   DATE/TIME: 2006-05-01 18:50:05   WHO: liangz

 Po   = 1 bar    =   100 kPa          Mixture: 30%H2+70%N2O
 CHAPMAN JOUGUET VALUES:
 Ucj = 1920.9 m/s                     Activation Energy =
 Pcj = 25.528 bar = 2.553 MPa         Prefl   = 63.178 bar = 6.318 MPa
 ZSigma = 0.125 mm                    MaxTempGrad = 0.123 mm
 CONSTANT PRESSURE, CONSTANT VOLUME COMBUSTION:
 Pcv = 12.956 bar = 1.296 MPa         c_cv    = 1017.5 m/s
 c_isobar = 937.4 m/s               Sigma   = 10.9

 #######  A) Prep & Vac ################################################
__ 1  vac pump, heat exchanger on
__    open hand valve, turn on gas key, evacuate line, turn off gas key
__    open bottlefarm valves.
__ 2  open V1, V2, V3, V5, V6,  Pressure < 50 mtorr
__ 3  Close V6, check leak rate, zero Heise guage
__ 4  Check position of ROTARY VALVE, zero AMPS
__ 5  Close door to room and DONT ENTER ROOM ANYMORE
__ 6  Turn on WARNING LIGHT

 #######  B) Filling    ################################################
__ 7  Turn on Gas Key switch
__ 8 Close V5
__ 9  Evacuate fill line:  Press and hold  VACCUUM  and  FAST FILL
__ 10 Pressurize line to experiment: Gas-flow switch and FAST FILL
__ 11 Open V5 and fill till desired pressure (last column)
Spec   MolFr     MolFrN    PartP(KPa)    acc(kPa)    P_got(kPA)  MolF_got
 H2    17.000     0.170     17.00       17.000       17.0         0.170
 N2O   83.000     0.830     83.00       100.000      100.0        0.830
__     LOOP through steps 8-11 for all gases
__ 12 Close V5, Evacuate fill line: Press and hold VACCUUM and FAST FILL
__ 13 Turn off Gas key switch

 ######## C) Circulate  ############################################
__ 14 Close V1
__ 15 Run circulation pump for 5 min.  start time: ____:____
__      final pressure:      99.98 kPa        (open and close V1)
__      final temperture:    23.5 C
__ 16 Close V2 , V3
__ 17 CHECK ALL VALVES ARE CLOSED

   #######      D) Arm & fire ###############################################
__ 18 Check sensor and trigger settings and shotnumber on DAS
__ 19 ARM DAS
__ 20 ! CHECK ALL VALVES CLOSED !
__ 21 ARM glow-plug
__ 22 FIRE
__ 23 Switch of glow-plug immediately after das triggered or 30 sec

   #######      E) Data       ###############################################
__ 24 check if data and setup file in shot dir
__ 25 Open V1 if temperature below 30C
__    post shot pressure:     112.22 kPa   post shot temperature:  28.5 C
__ 26 Open V2 , V3 , V6
__ 27 End of shot series: Close hand valves, Shut of gas key,
__    shut off gas bottle farm, turn off evacuation pump

 ####### COMMENTS ###################################################

With obstacles (BR=0.25), glow plug, 8 strain gauges and 8 pressure transducers.
```

B Tube setup

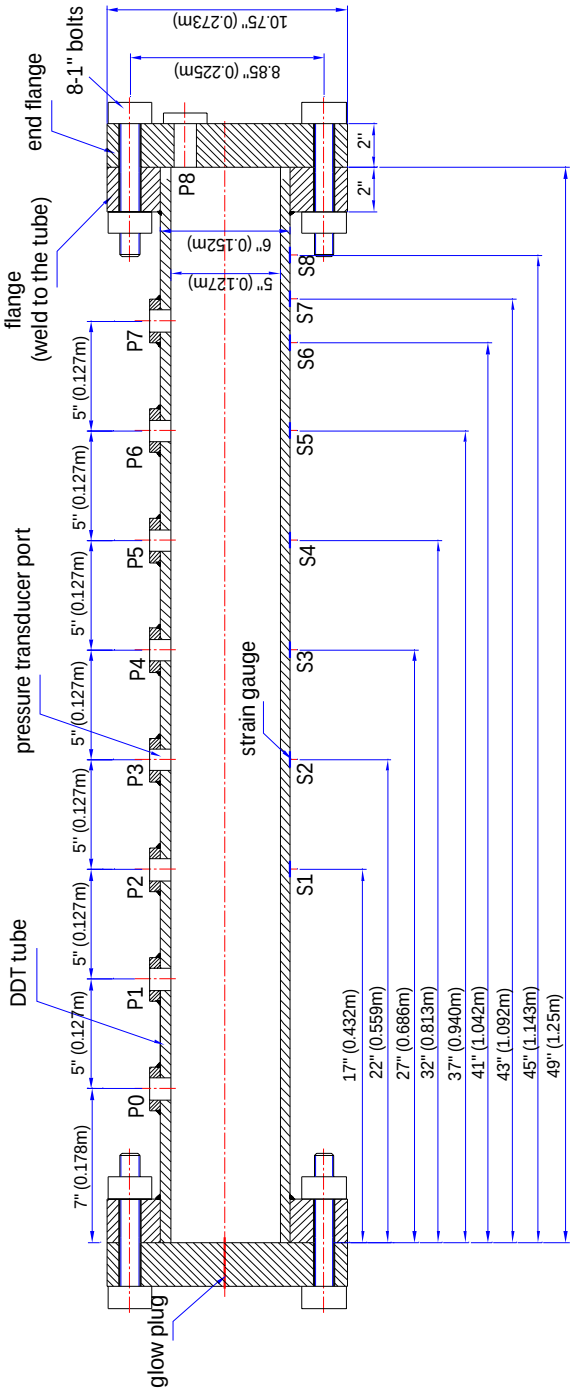

Figure 8: Tube setup for test series A.

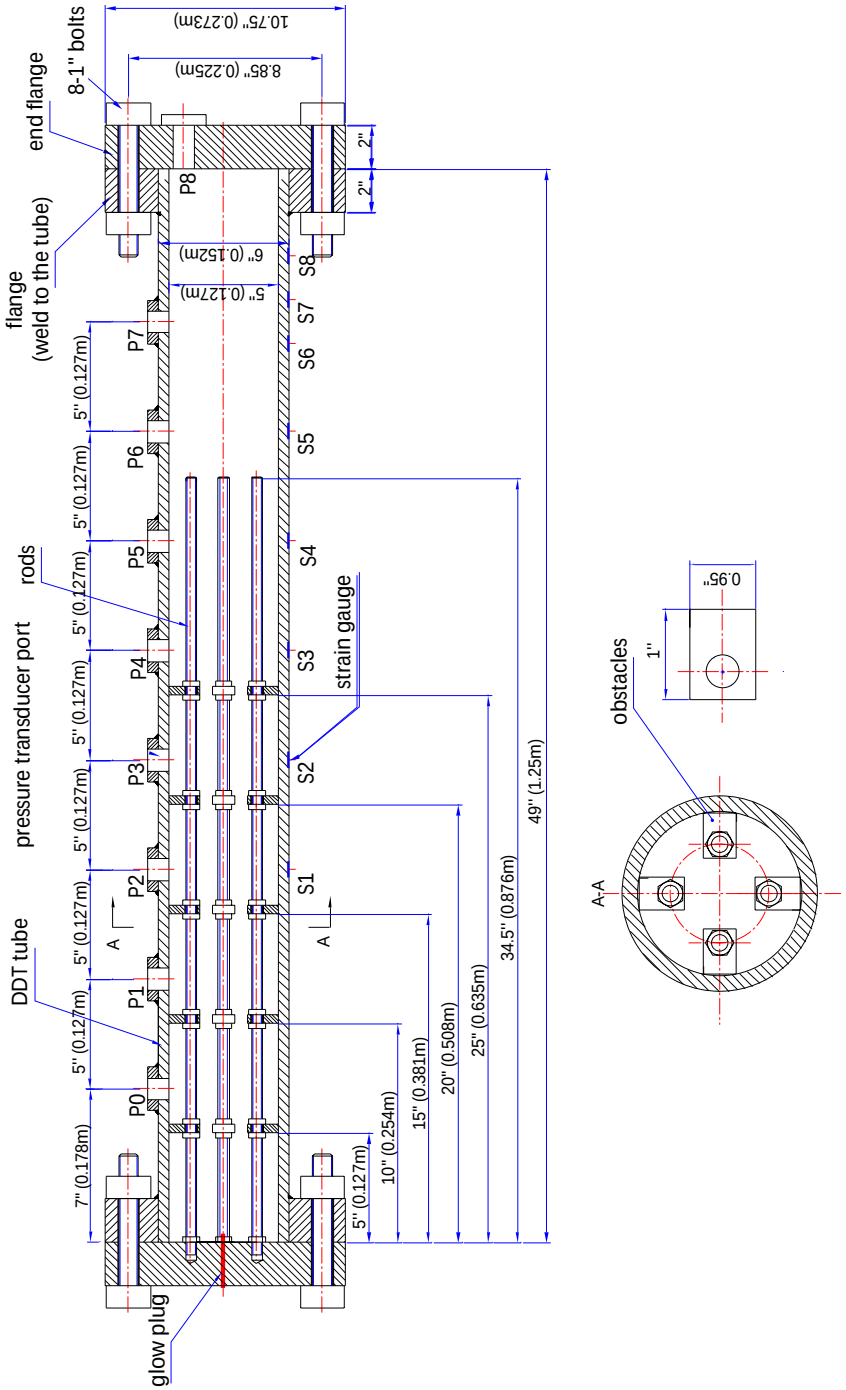

Figure 9: Tube setup for test series B.

C Pressure and strain history of shots 56-72

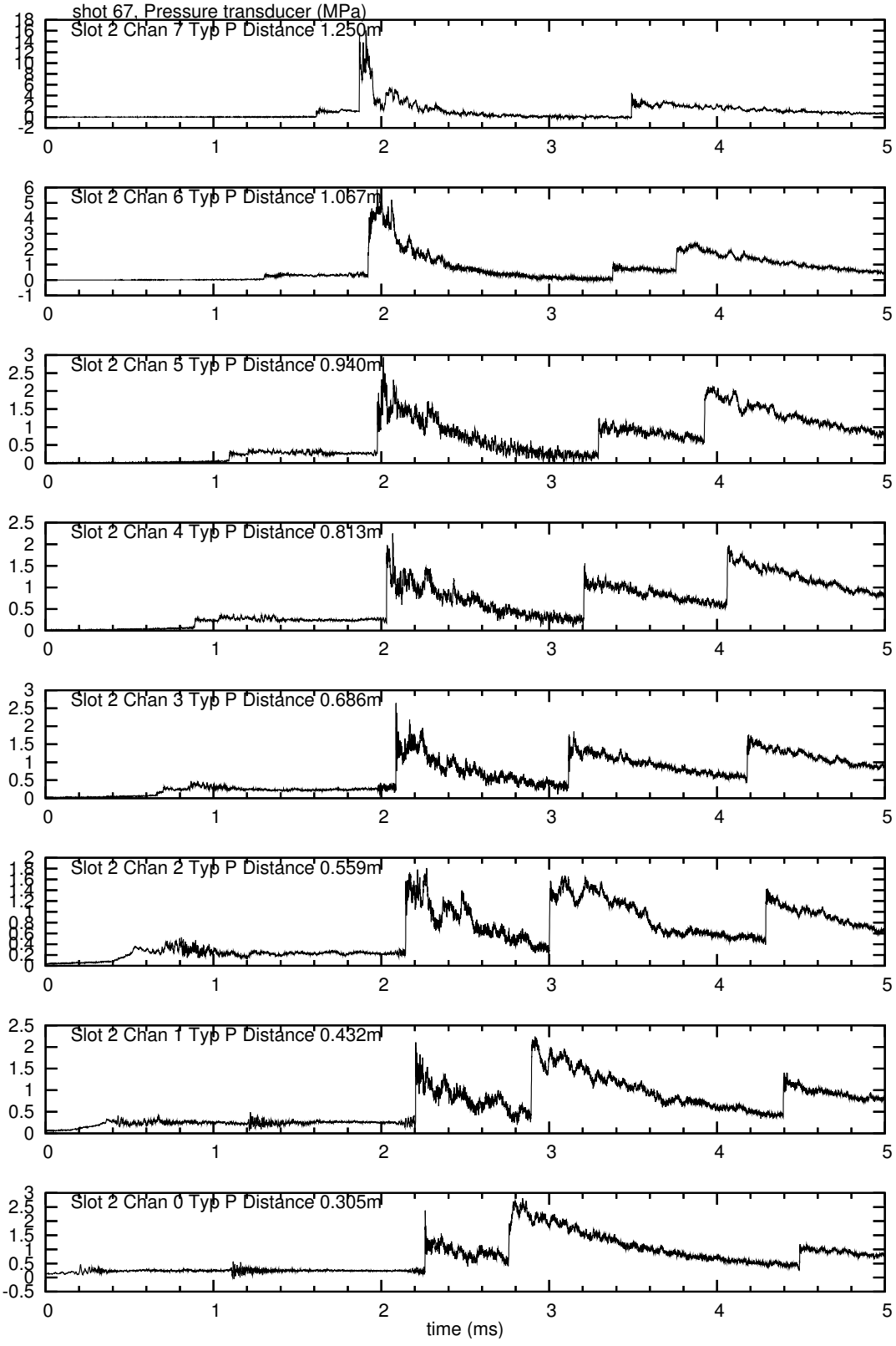

Figure 10: Pressure transducers, shot 67, 30% H_2, test series A, no obstacles.

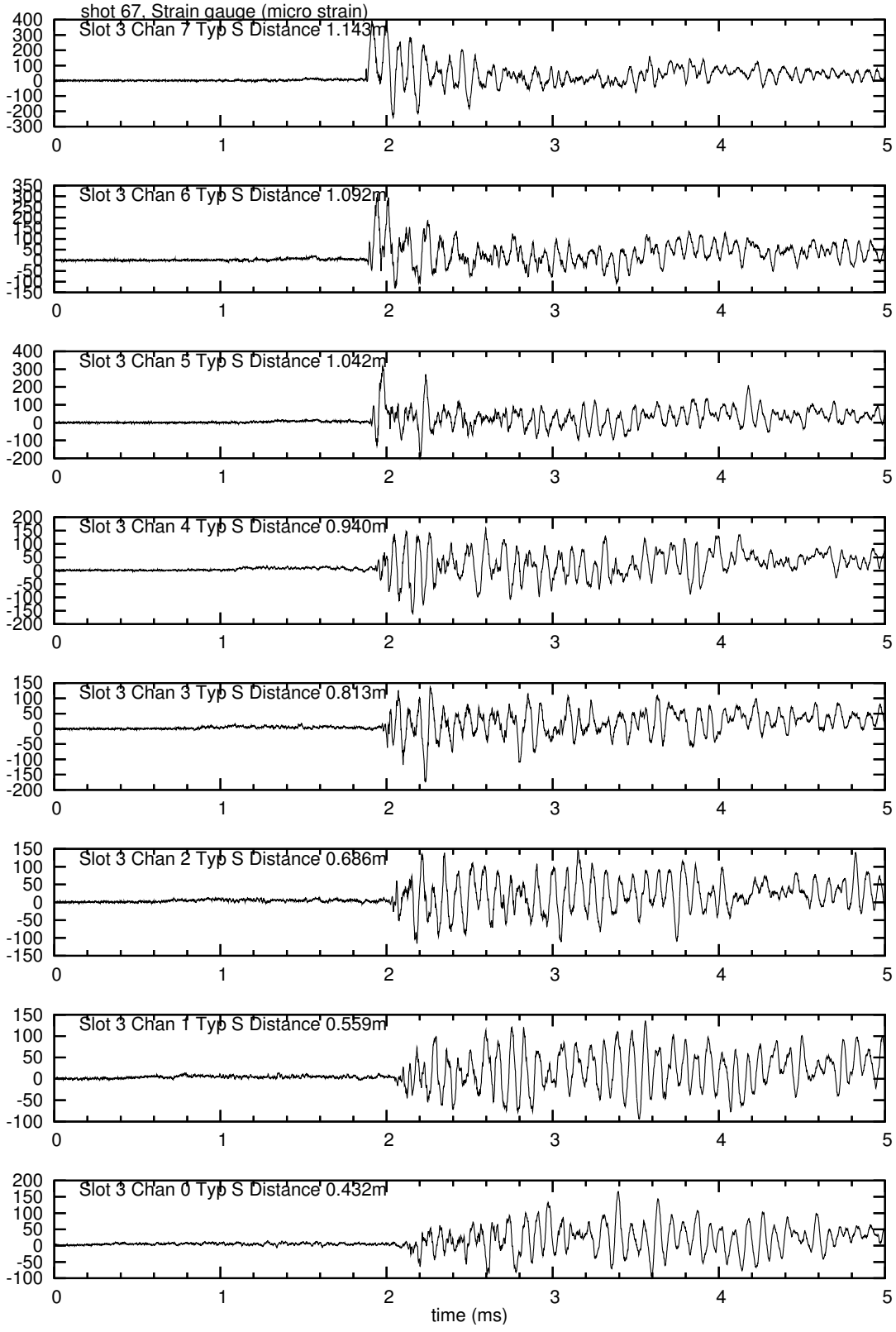

Figure 11: Strain gauges, shot 67, 30% H_2, test series A, no obstacles.

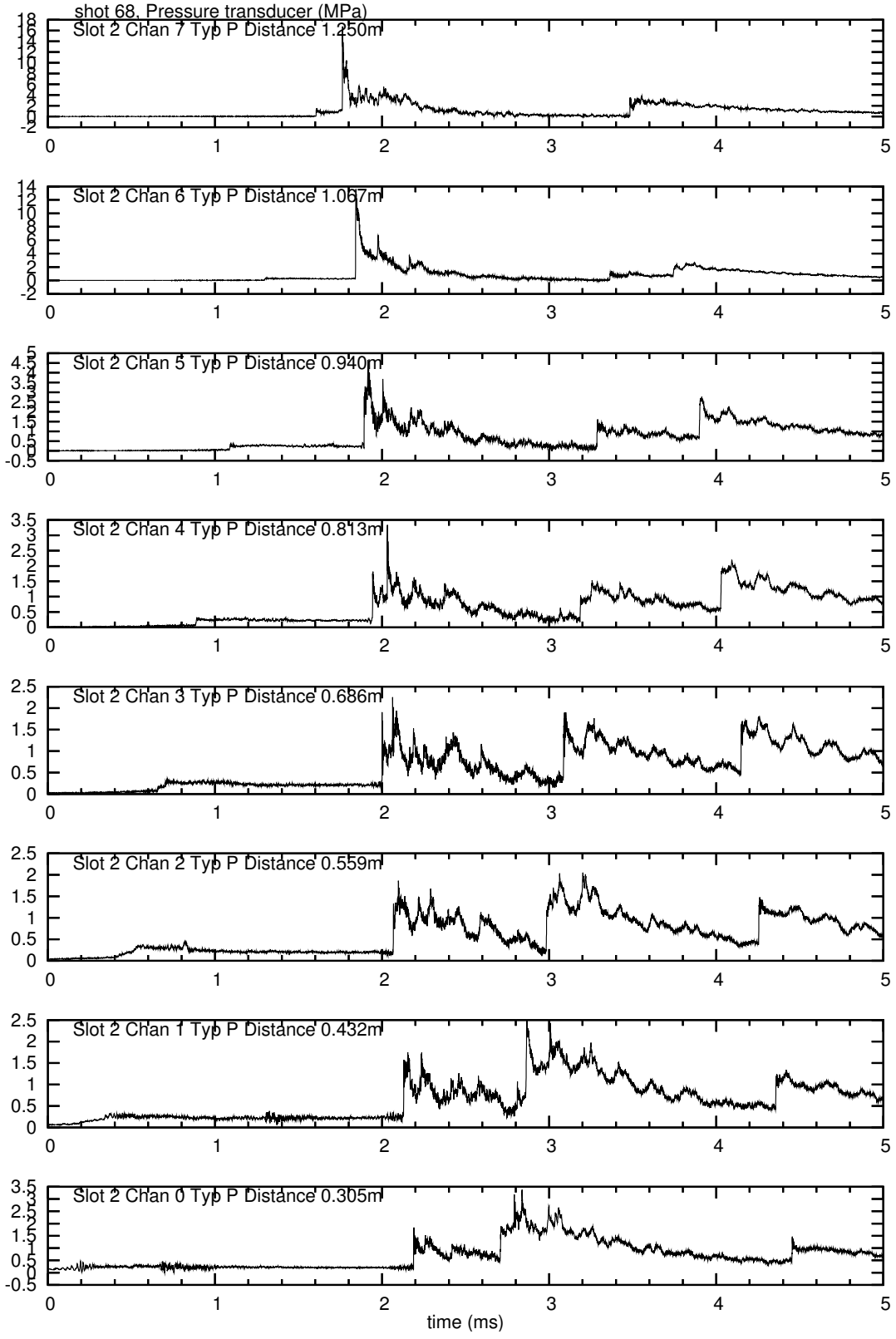

Figure 12: Pressure transducers, shot 68, 30% H_2, test series A, no obstacles.

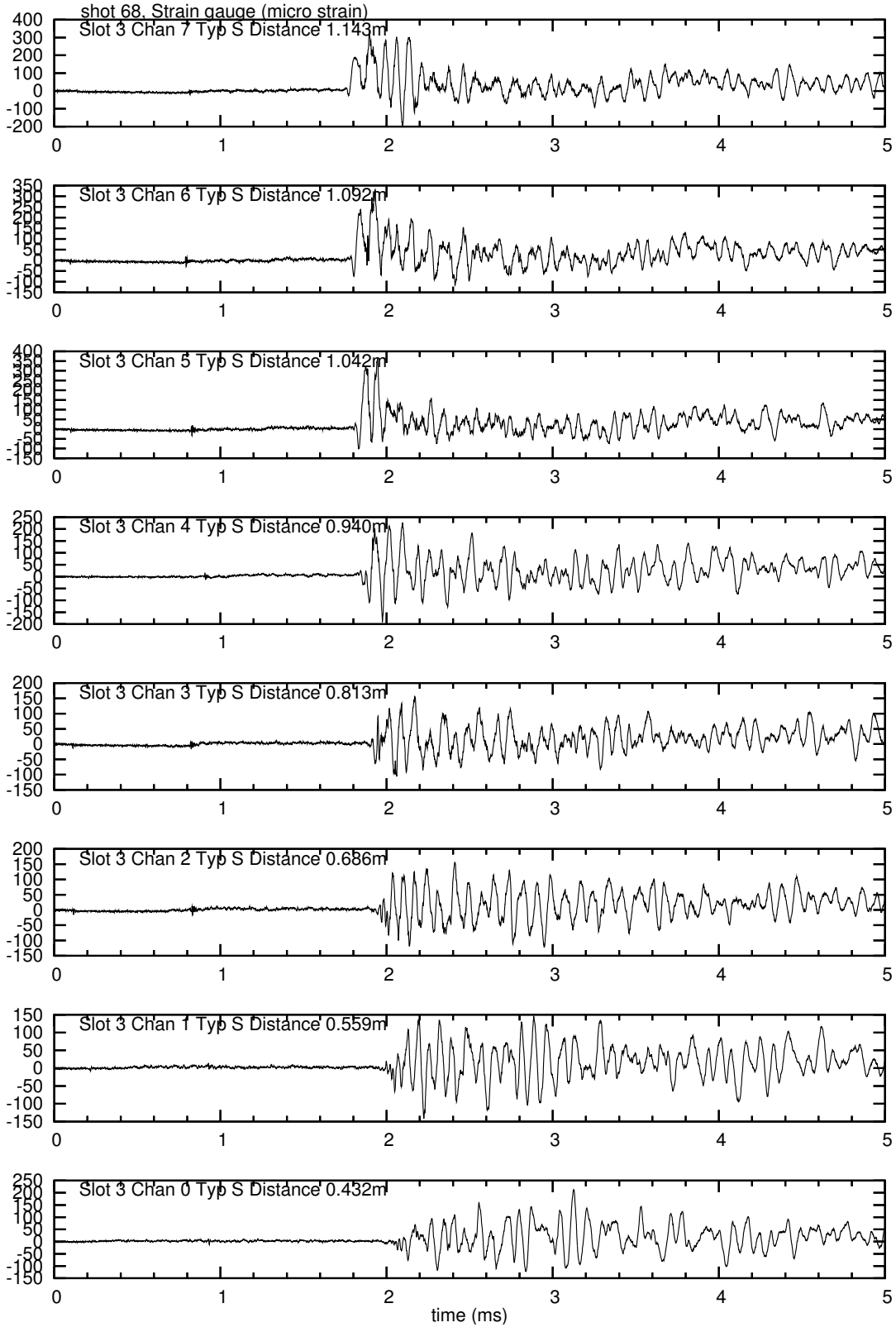

Figure 13: Strain gauges, shot 68, 30% H_2, test series A, no obstacles.

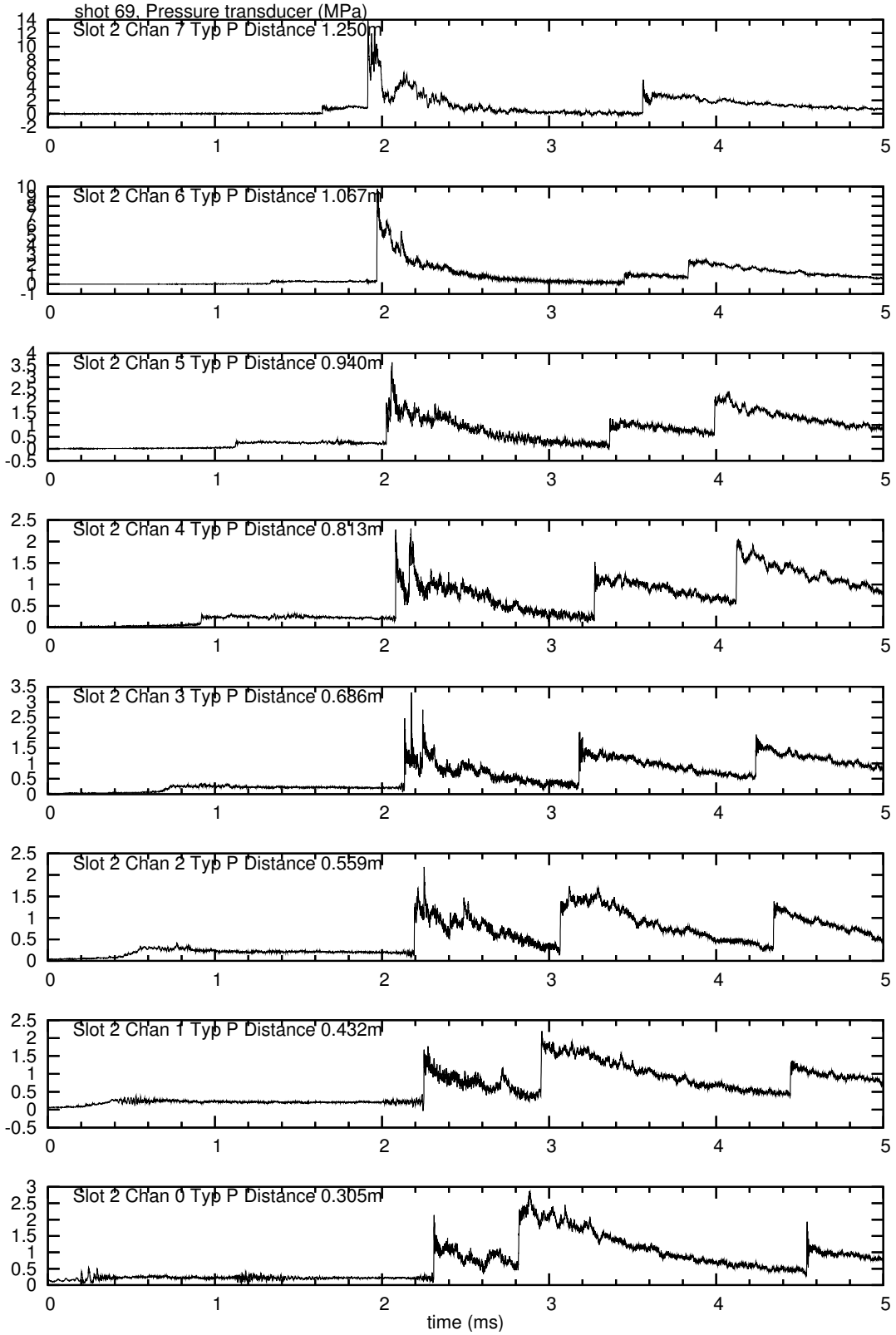

Figure 14: Pressure transducers, shot 69, 30% H_2, test series A, no obstacles.

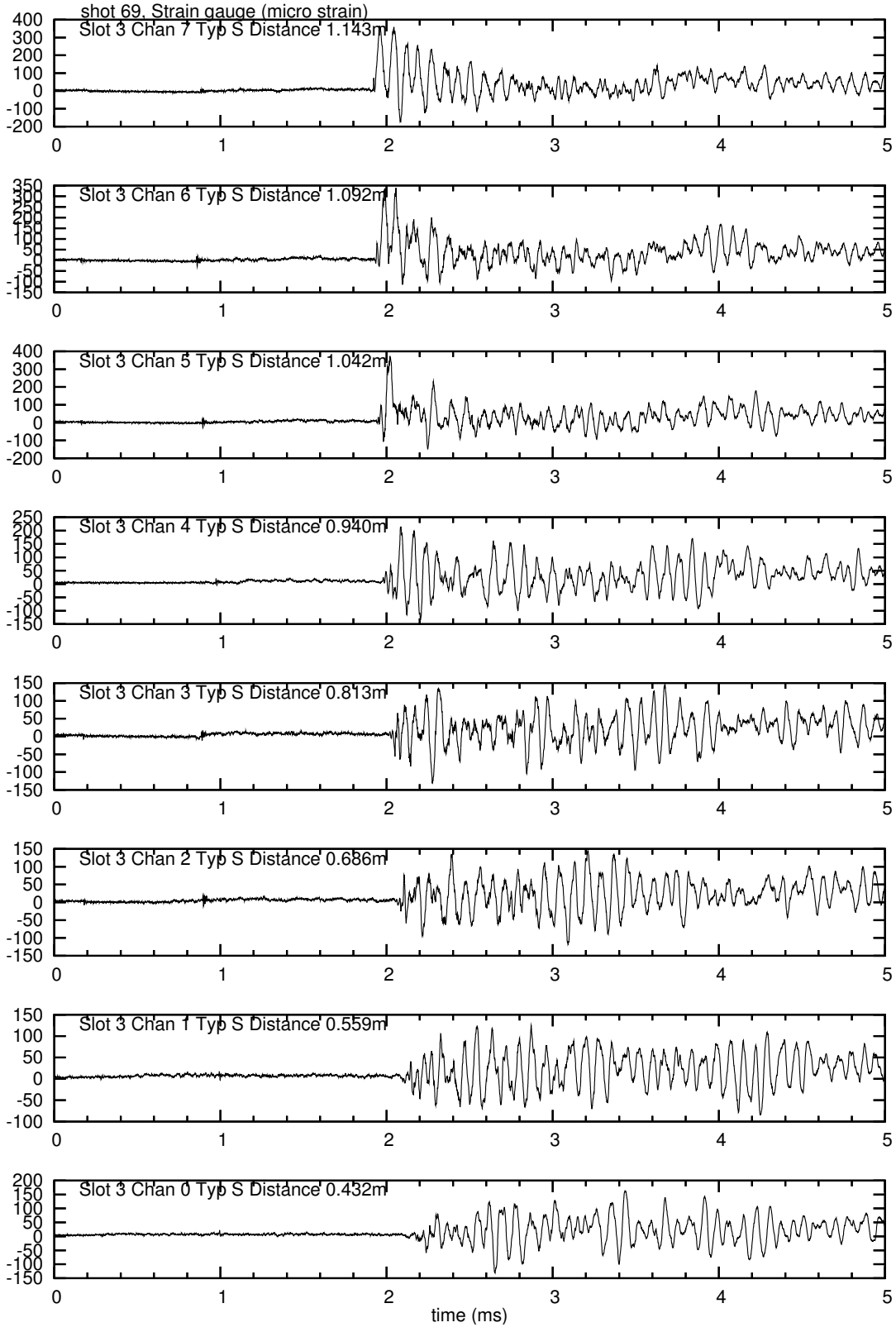

Figure 15: Strain gauges, shot 69, 30% H_2, test series A, no obstacles.

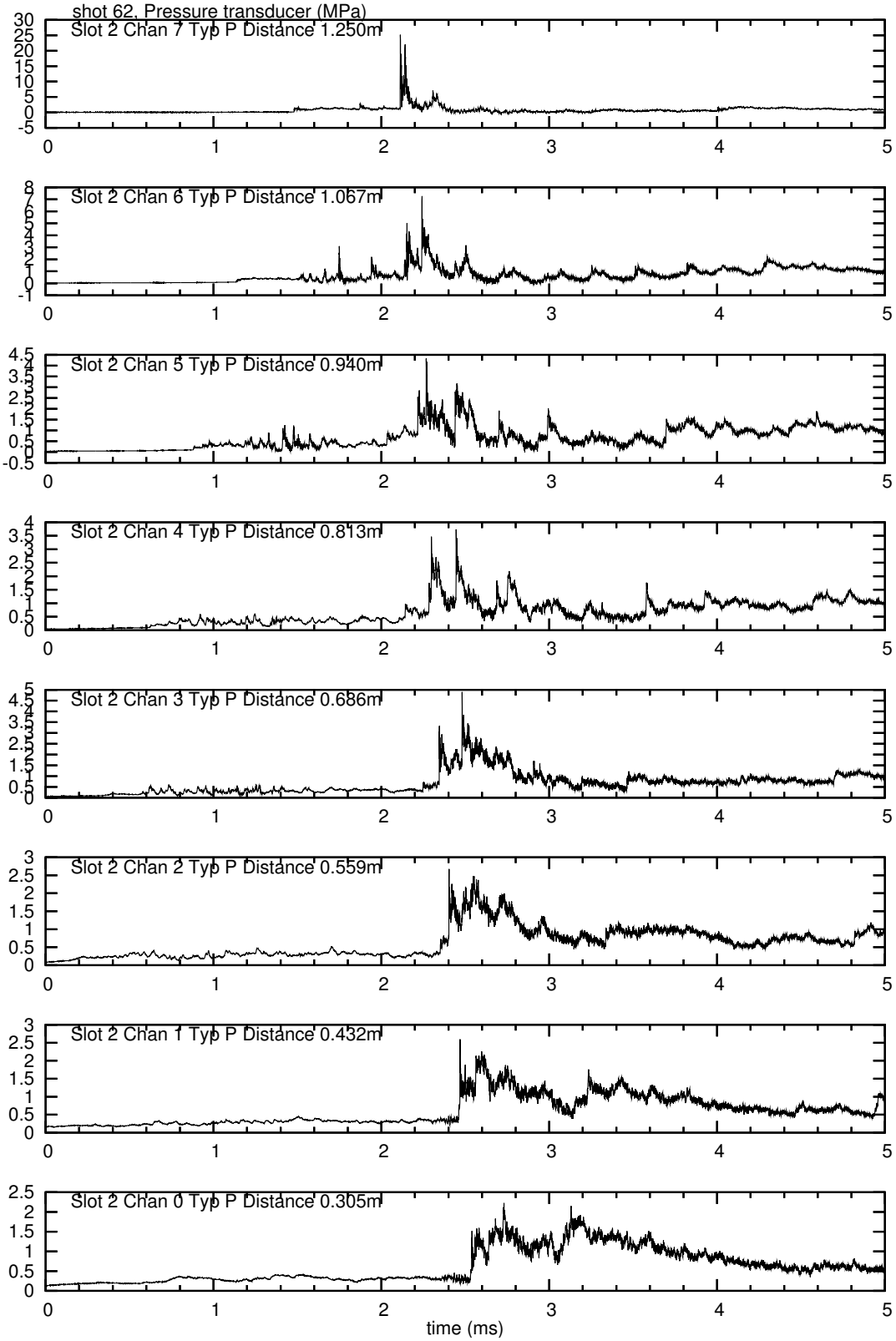

Figure 16: Pressure transducers, shot 62, 15% H_2, test series B, with obstacles.

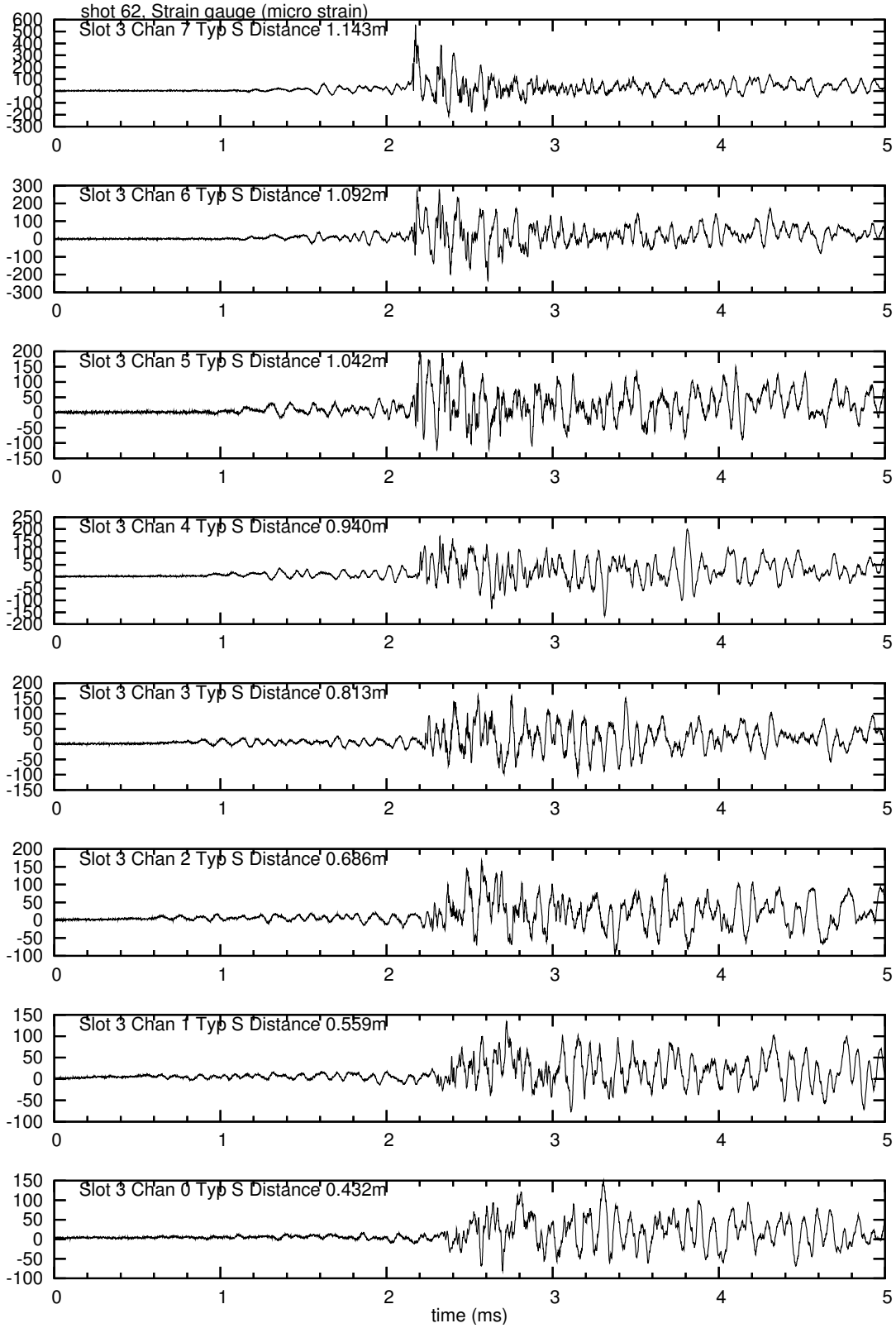

Figure 17: Strain gauges, shot 62, 15% H_2, test series B, with obstacles.

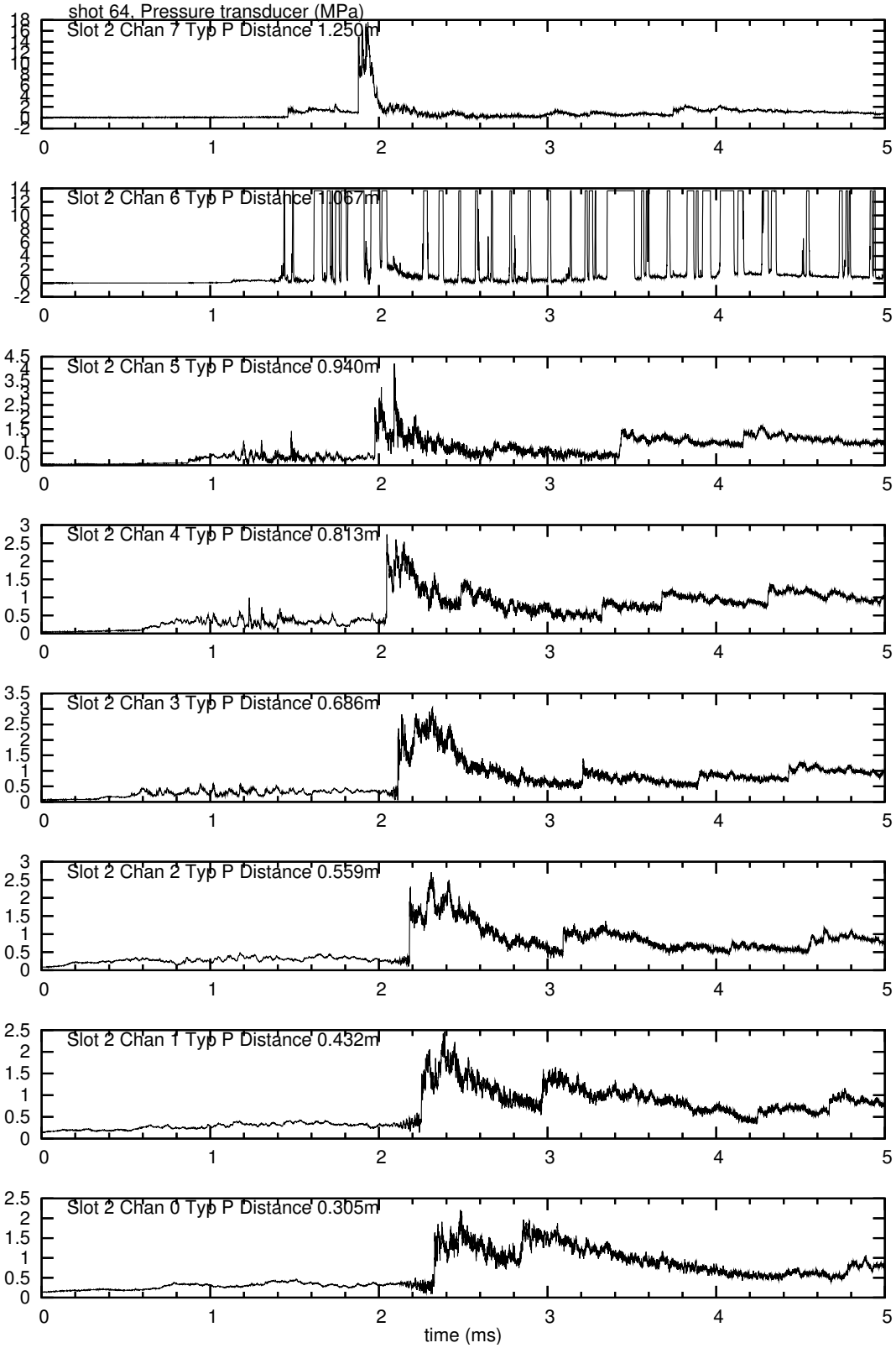

Figure 18: Pressure transducers, shot 64, 15% H_2, test series B, with obstacles.

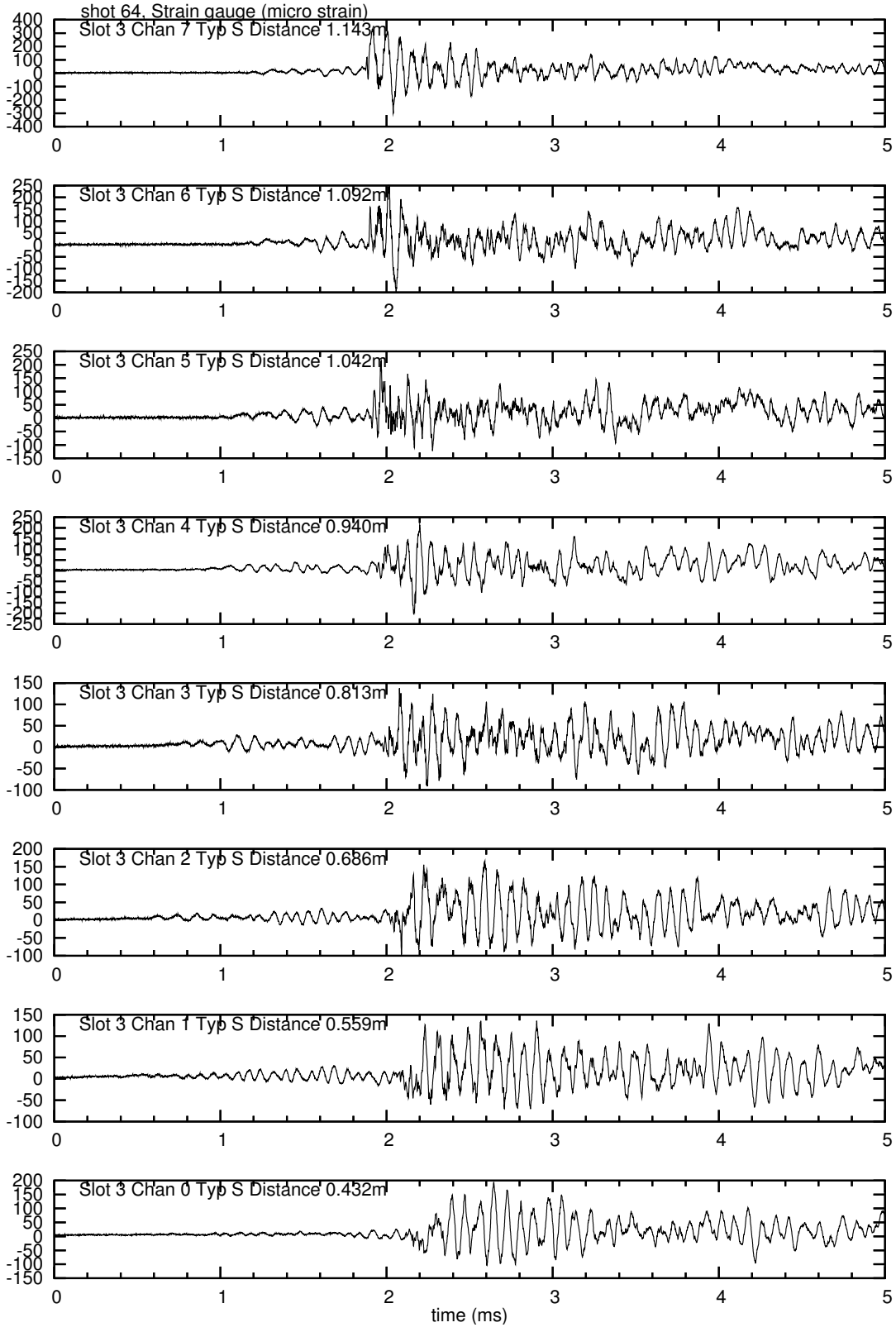

Figure 19: Strain gauges, shot 64, 15% H_2, test series B, with obstacles.

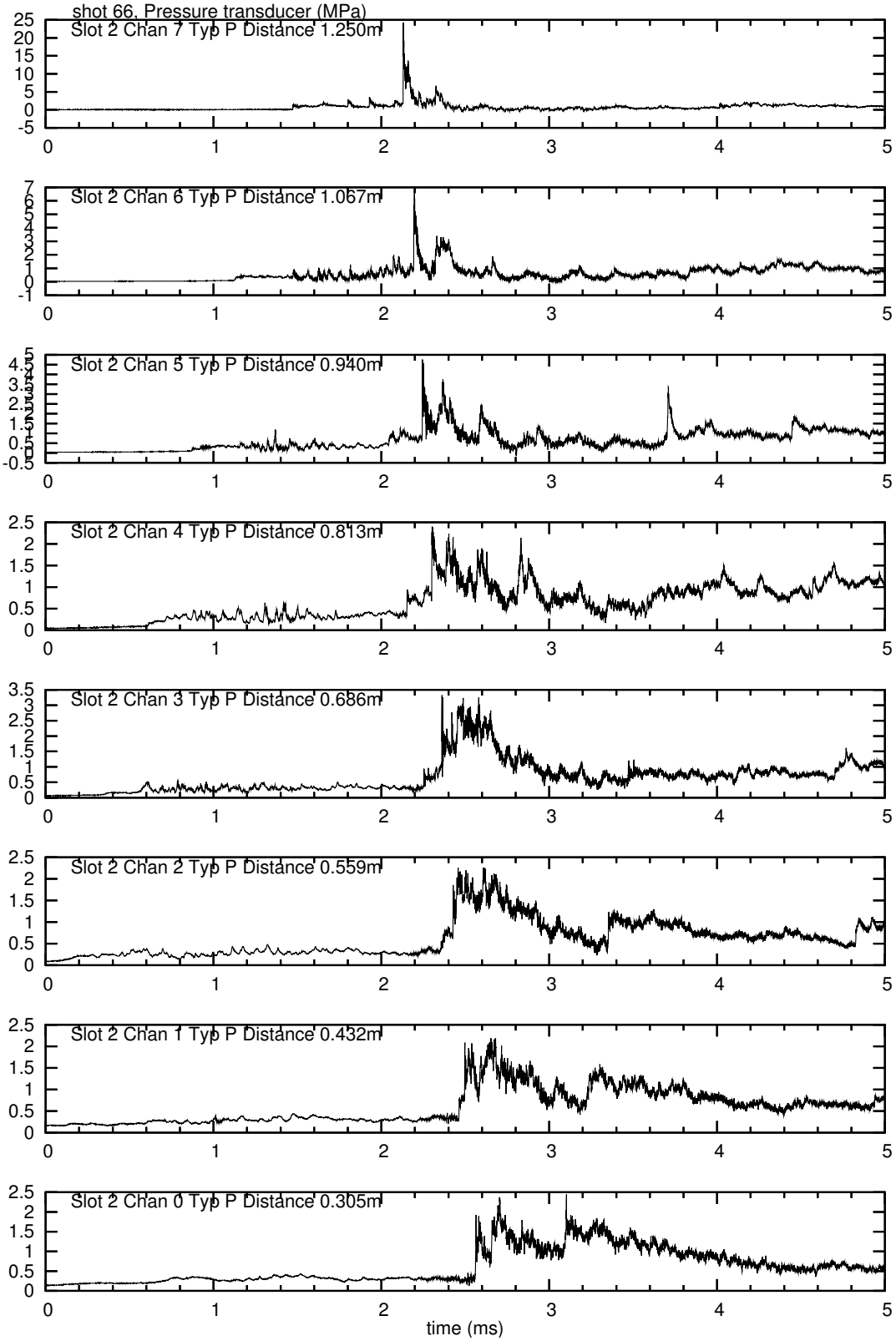

Figure 20: Pressure transducers, shot 66, 15% H_2, test series B, with obstacles.

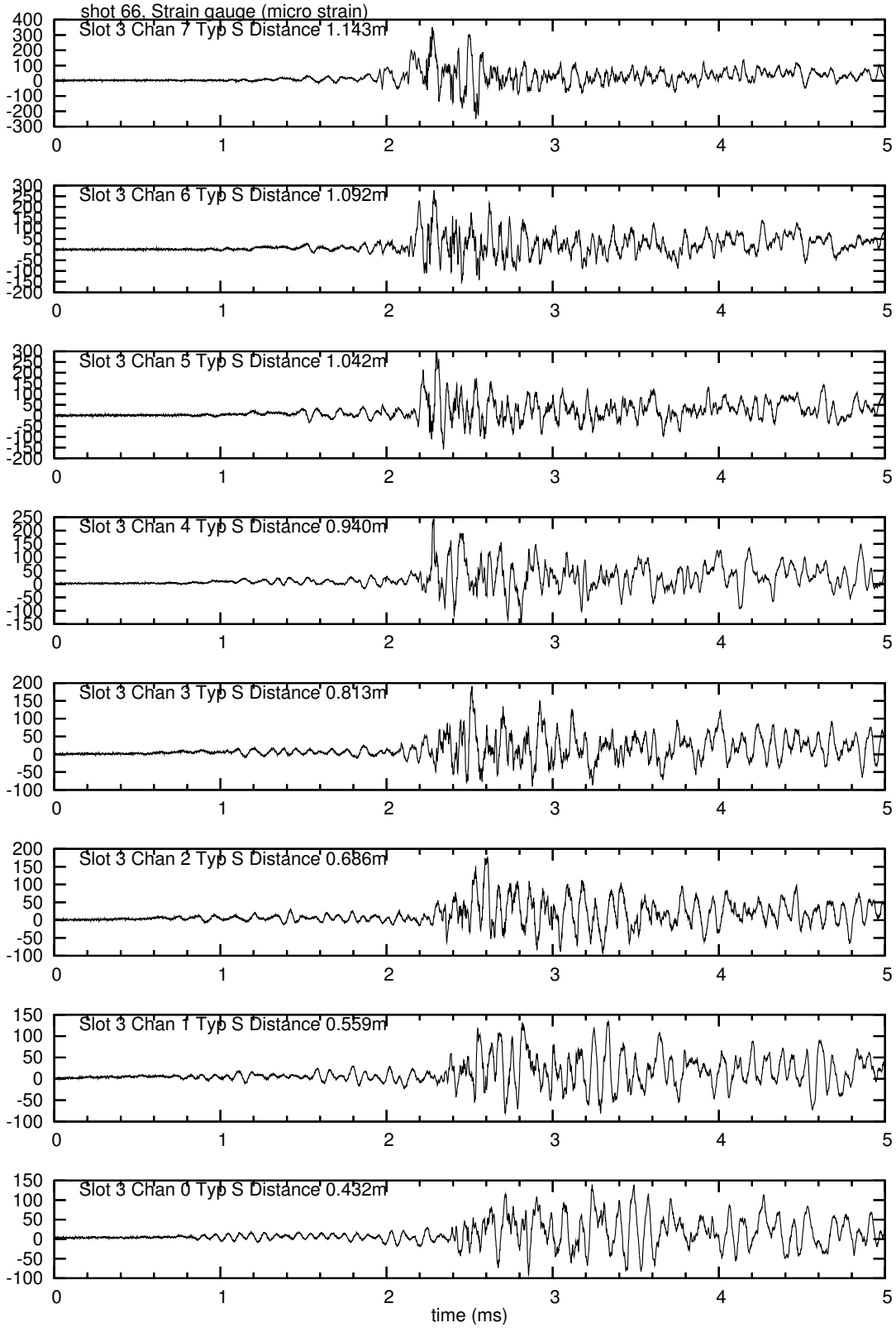

Figure 21: Strain gauges, shot 66, 15% H_2, test series B, with obstacles.

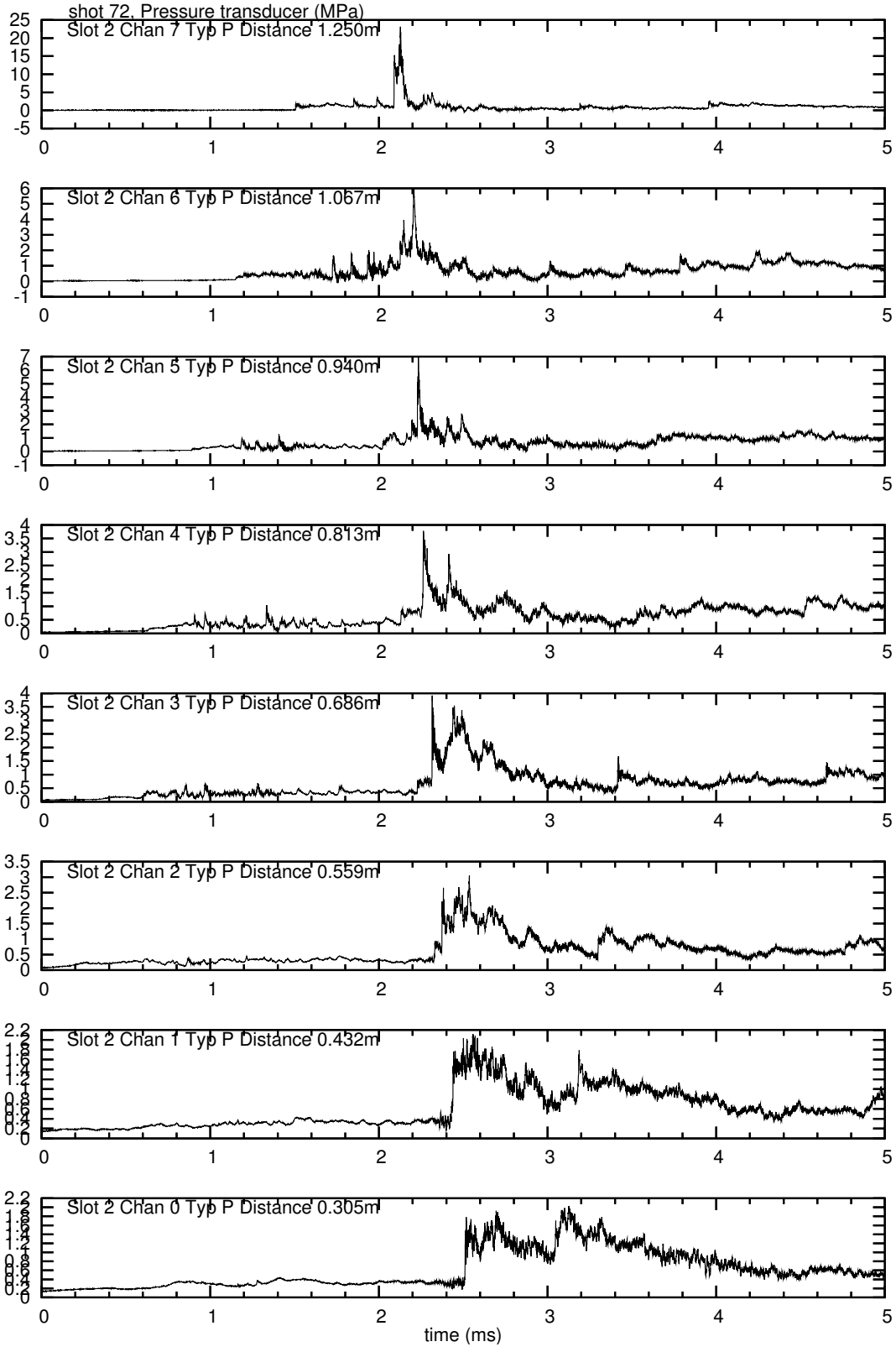

Figure 22: Pressure transducers, shot 72, 15% H_2, test series B, with obstacles.

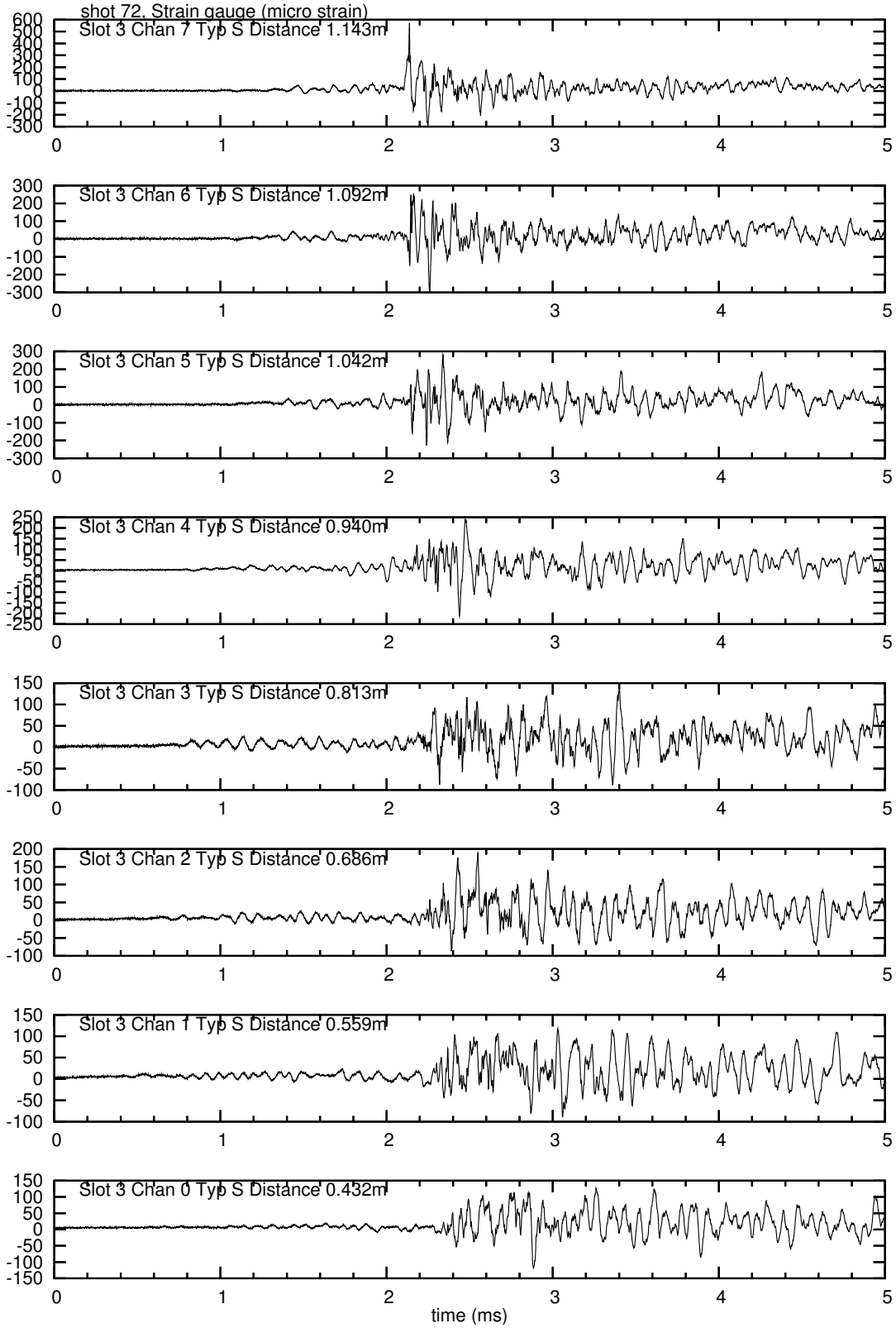

Figure 23: Strain gauges, shot 72, 15% H_2, test series B, with obstacles.

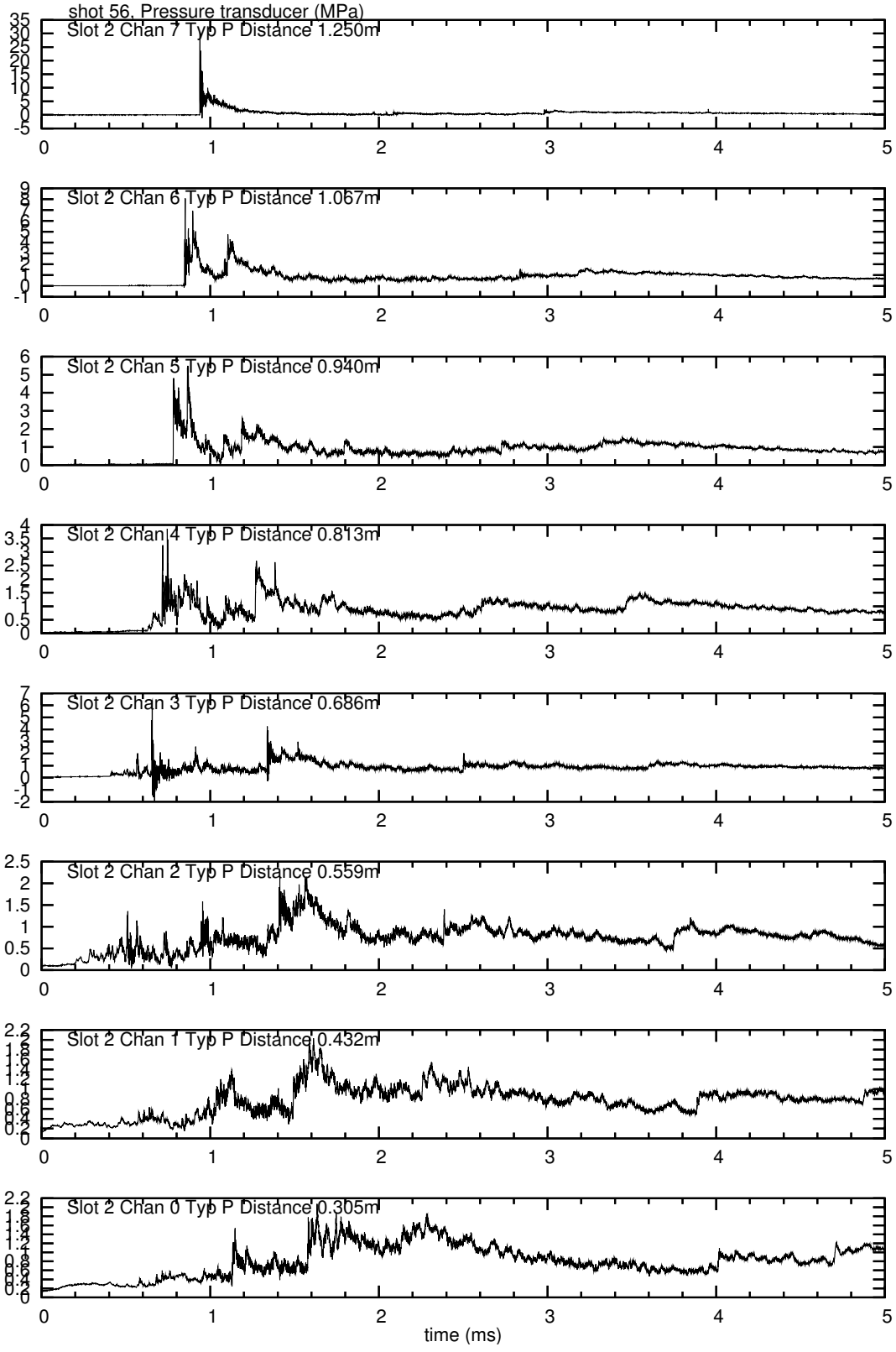

Figure 24: Pressure transducers, shot 56, 17% H_2, test series B, with obstacles.

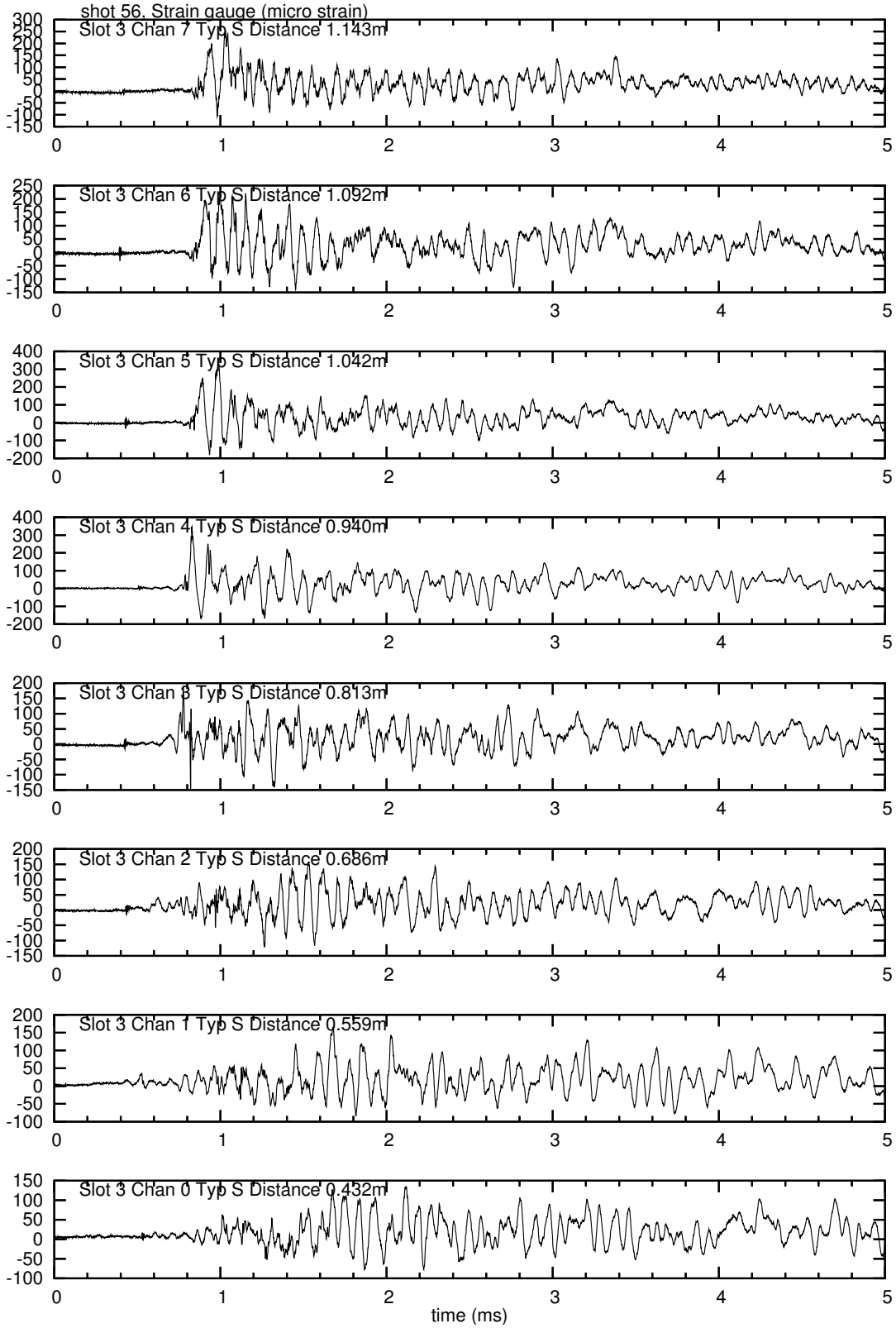

Figure 25: Strain gauges, shot 56, 17% H_2, test series B, with obstacles.

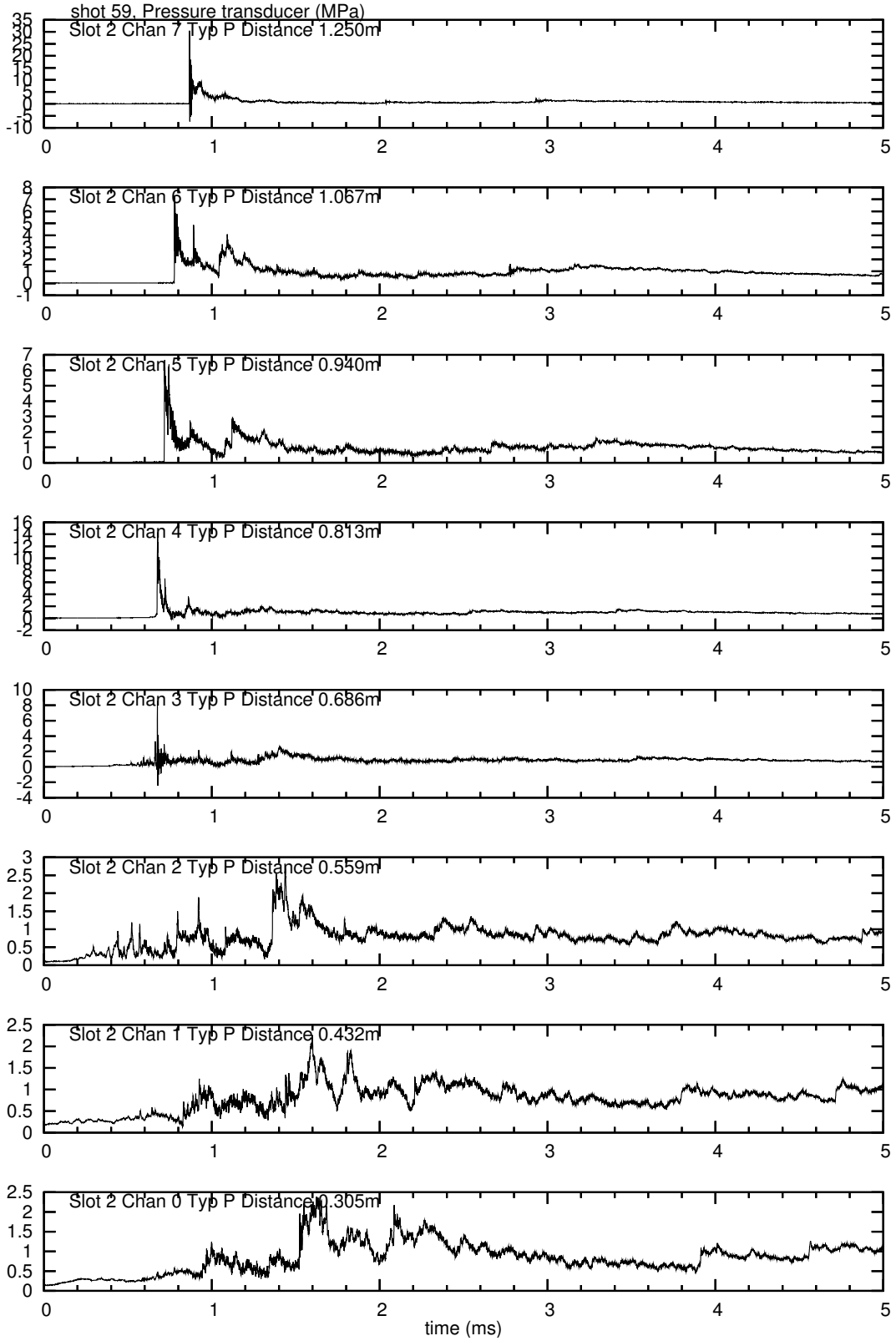

Figure 26: Pressure transducers, shot 59, 17% H_2, test series B, with obstacles.

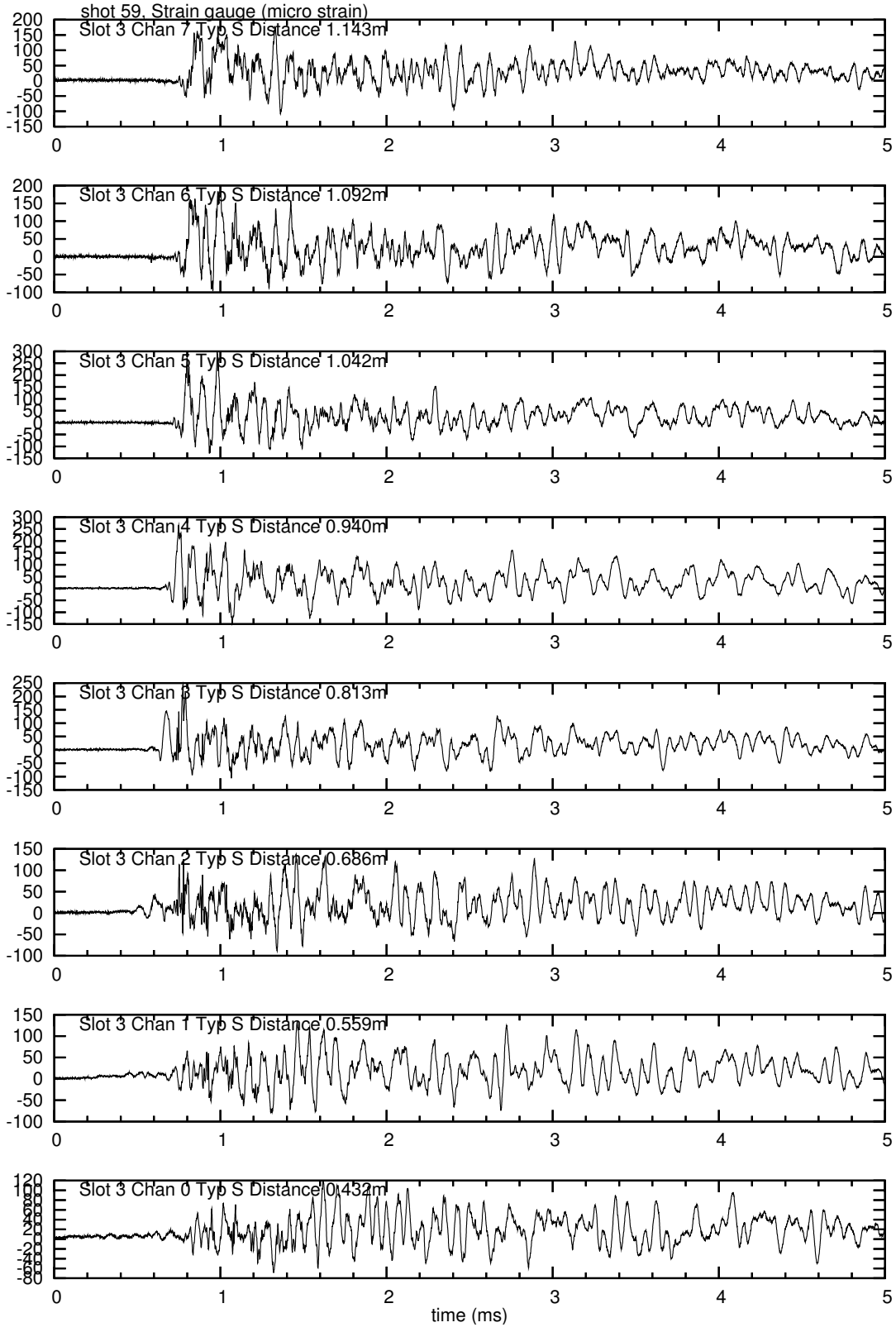

Figure 27: Strain gauges, shot 59, 17% H_2, test series B, with obstacles.

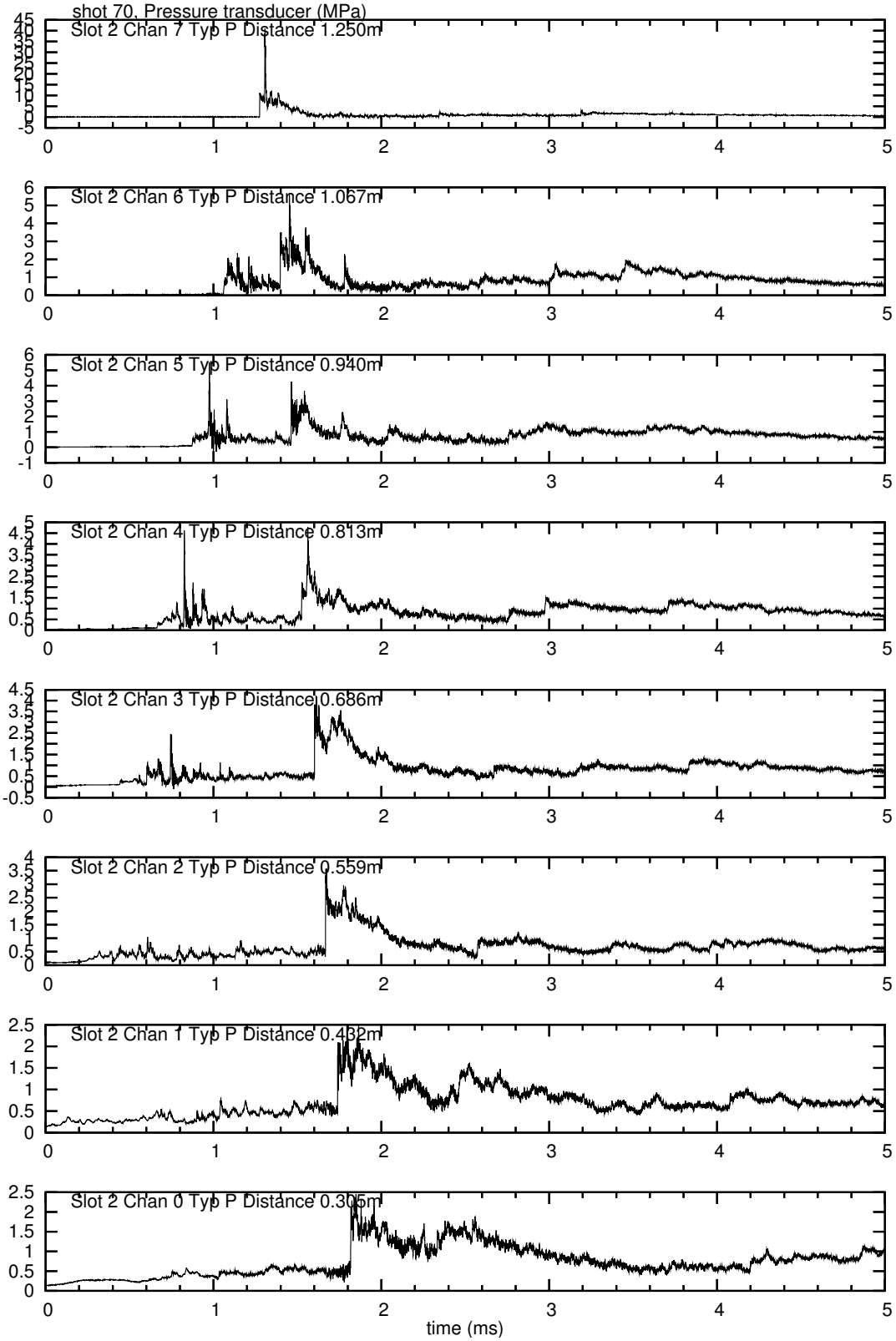

Figure 28: Pressure transducers, shot 70, 17% H_2, test series B, with obstacles.

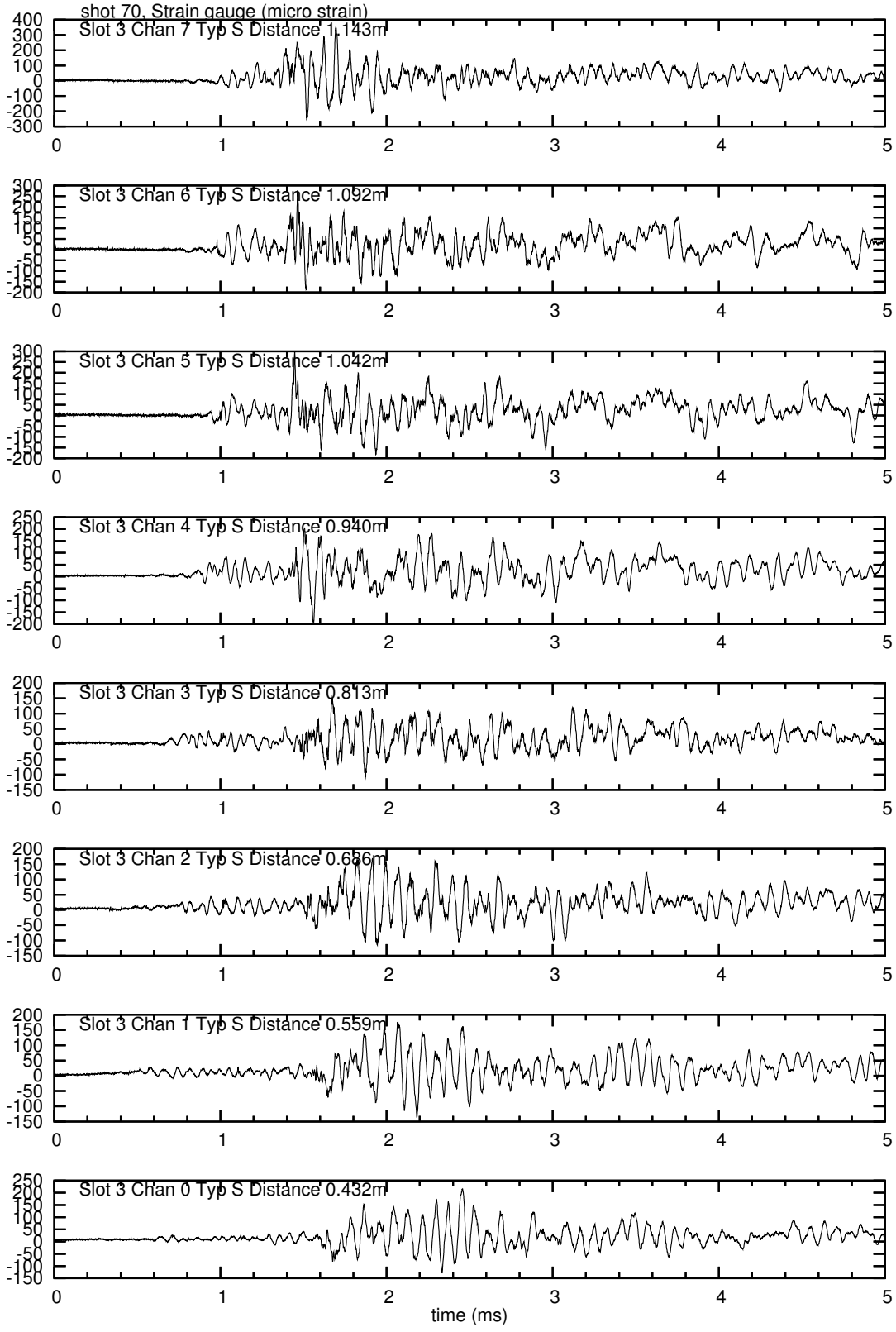

Figure 29: Strain gauges, shot 70, 17% H_2, test series B, with obstacles.

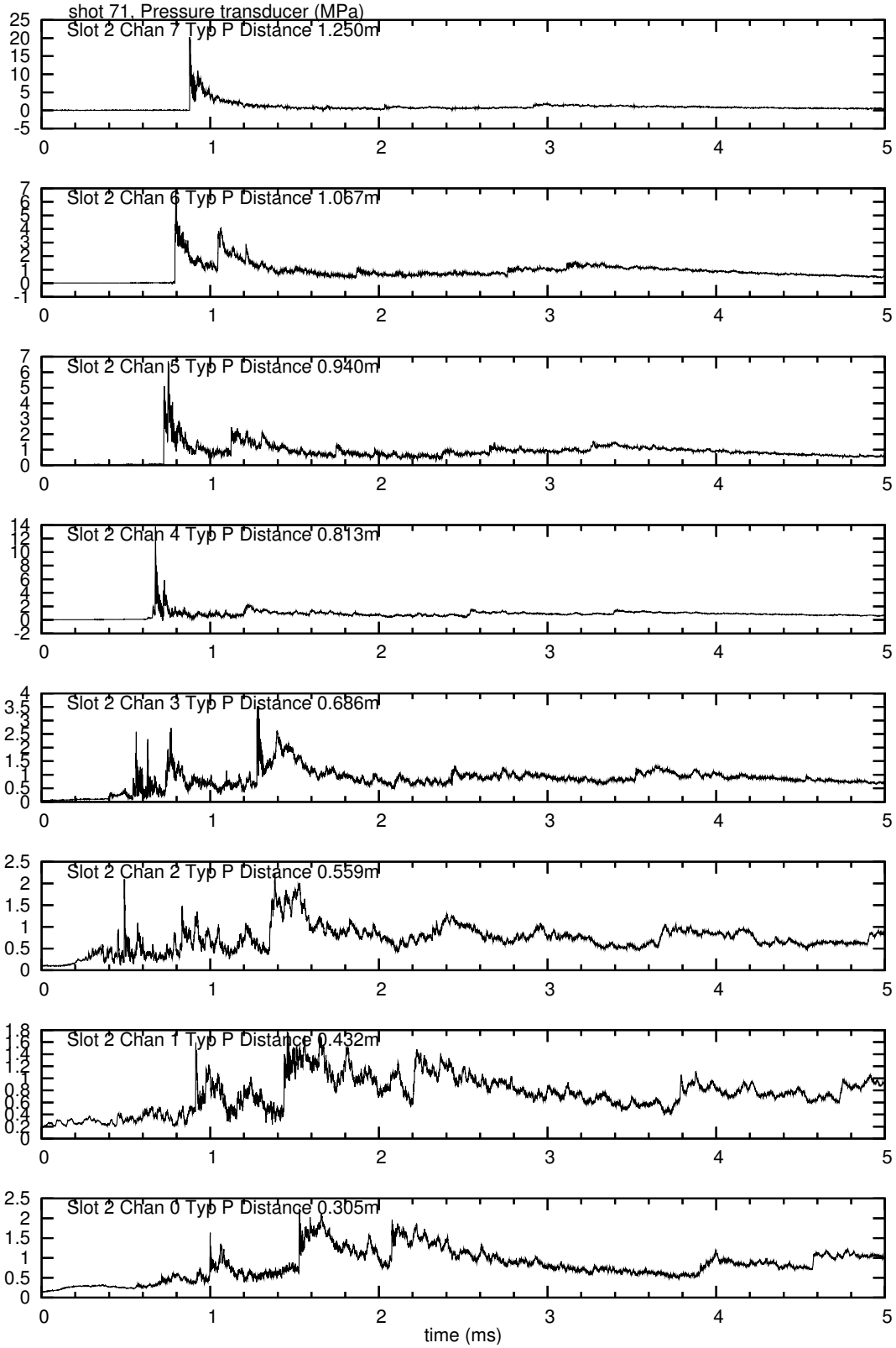

Figure 30: Pressure transducers, shot 71, 17% H_2, test series B, with obstacles.

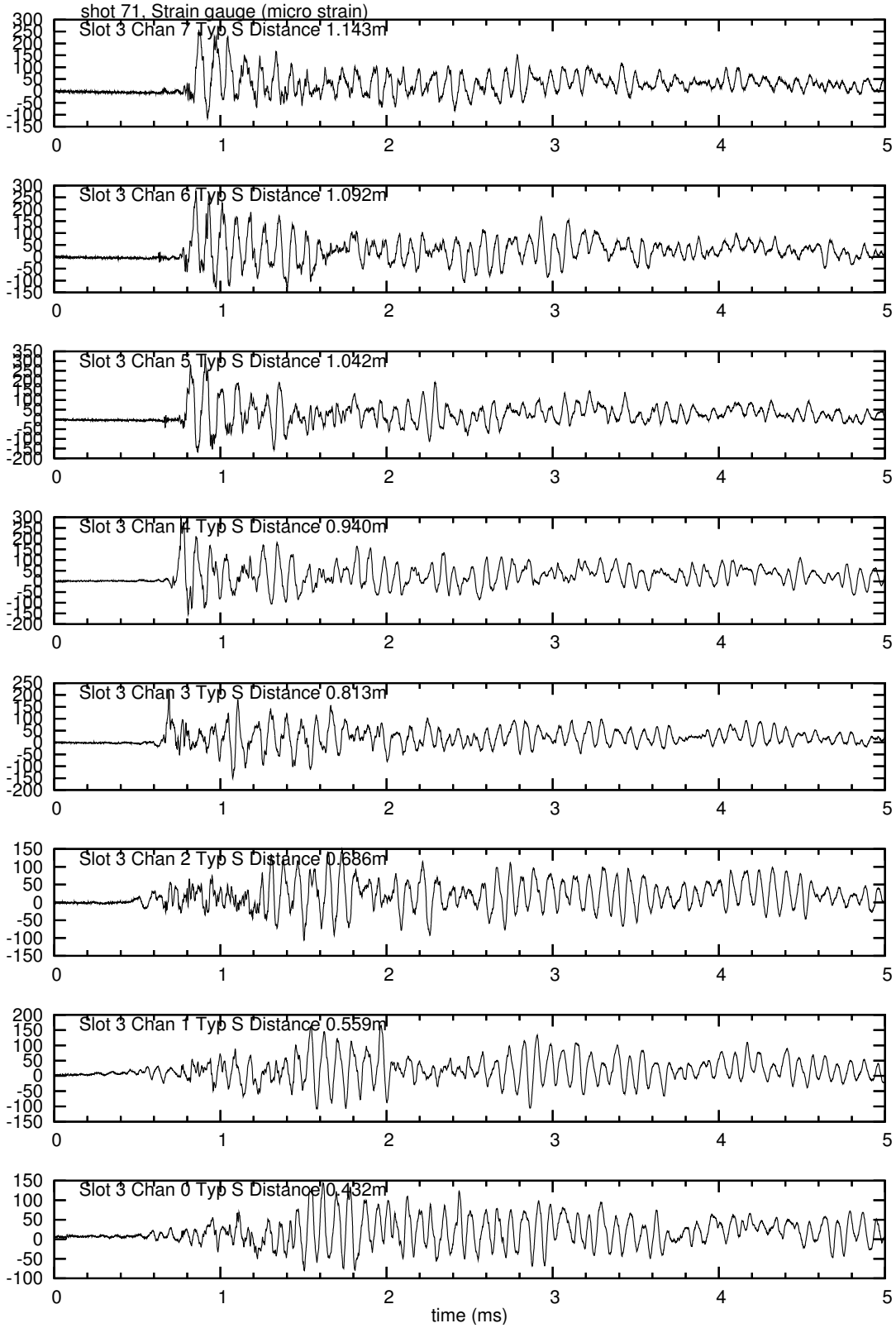

Figure 31: Strain gauges, shot 71, 17% H_2, test series B, with obstacles.

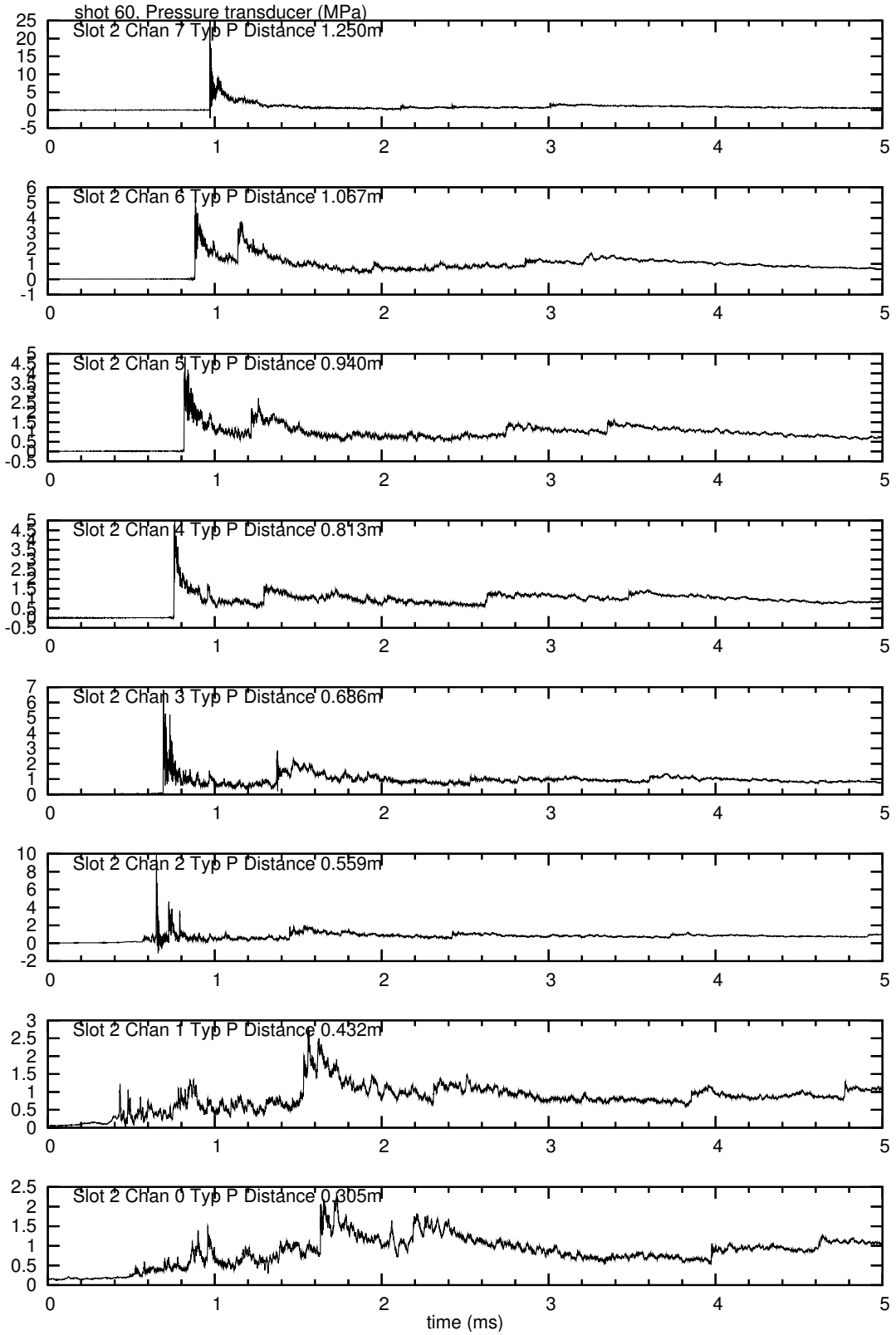

Figure 32: Pressure transducers, shot 60, 20% H_2, test series B, with obstacles.

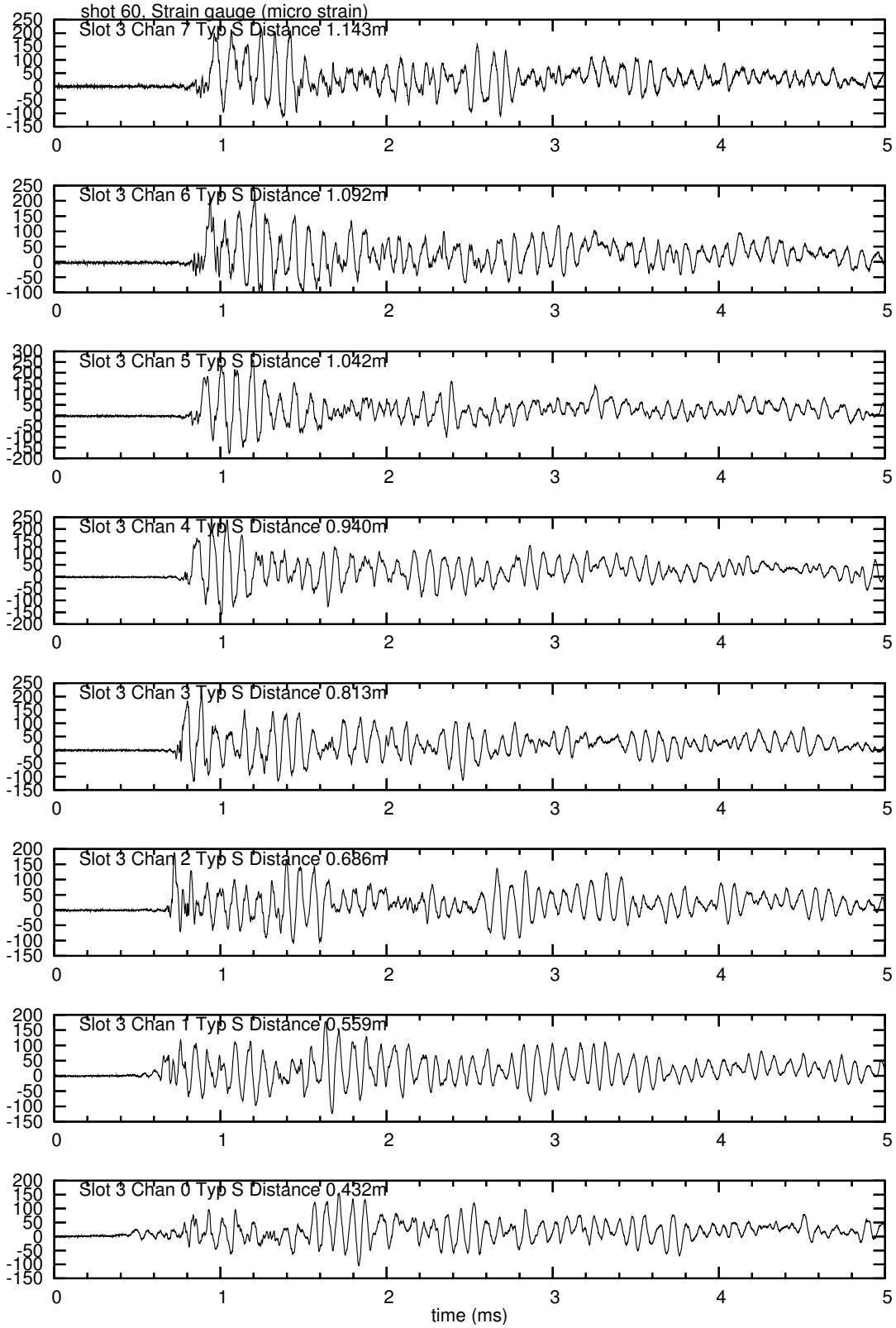

Figure 33: Strain gauges, shot 60, 20% H_2, test series B, with obstacles.

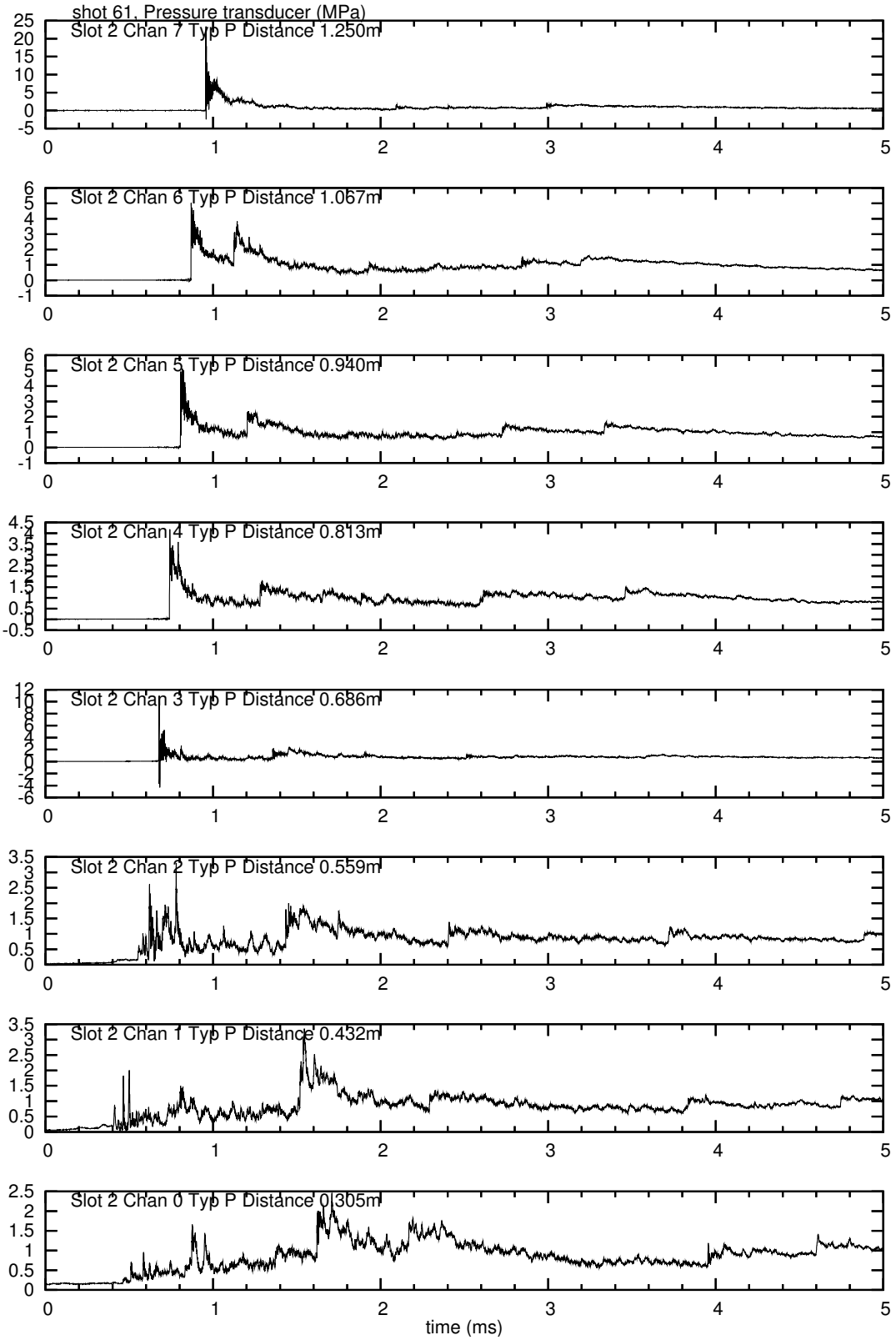

Figure 34: Pressure transducers, shot 61, 20% H_2, test series B, with obstacles.

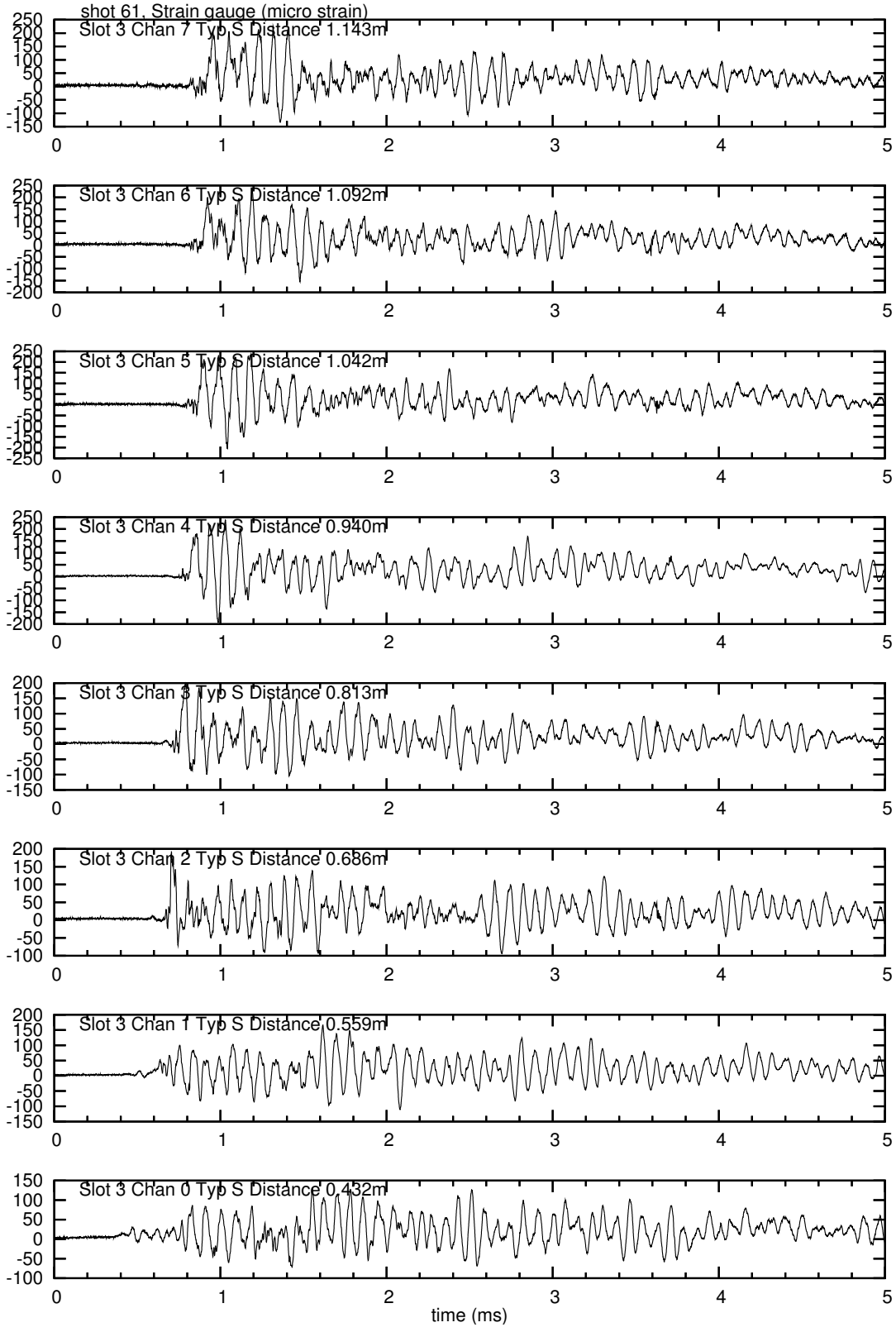

Figure 35: Strain gauges, shot 61, 20% H_2, test series B, with obstacles.

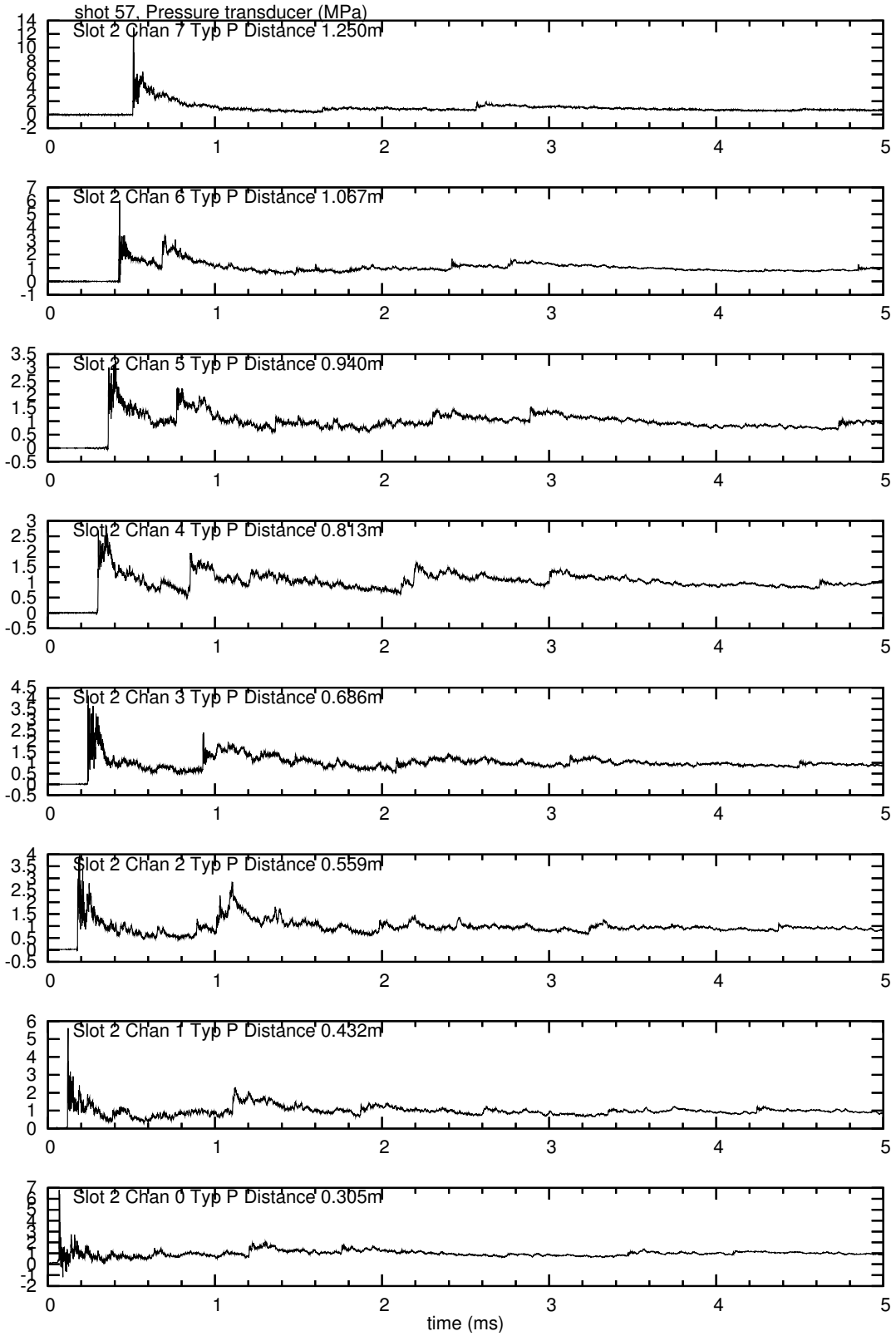

Figure 36: Pressure transducers, shot 57, 30% H_2, test series B, with obstacles.

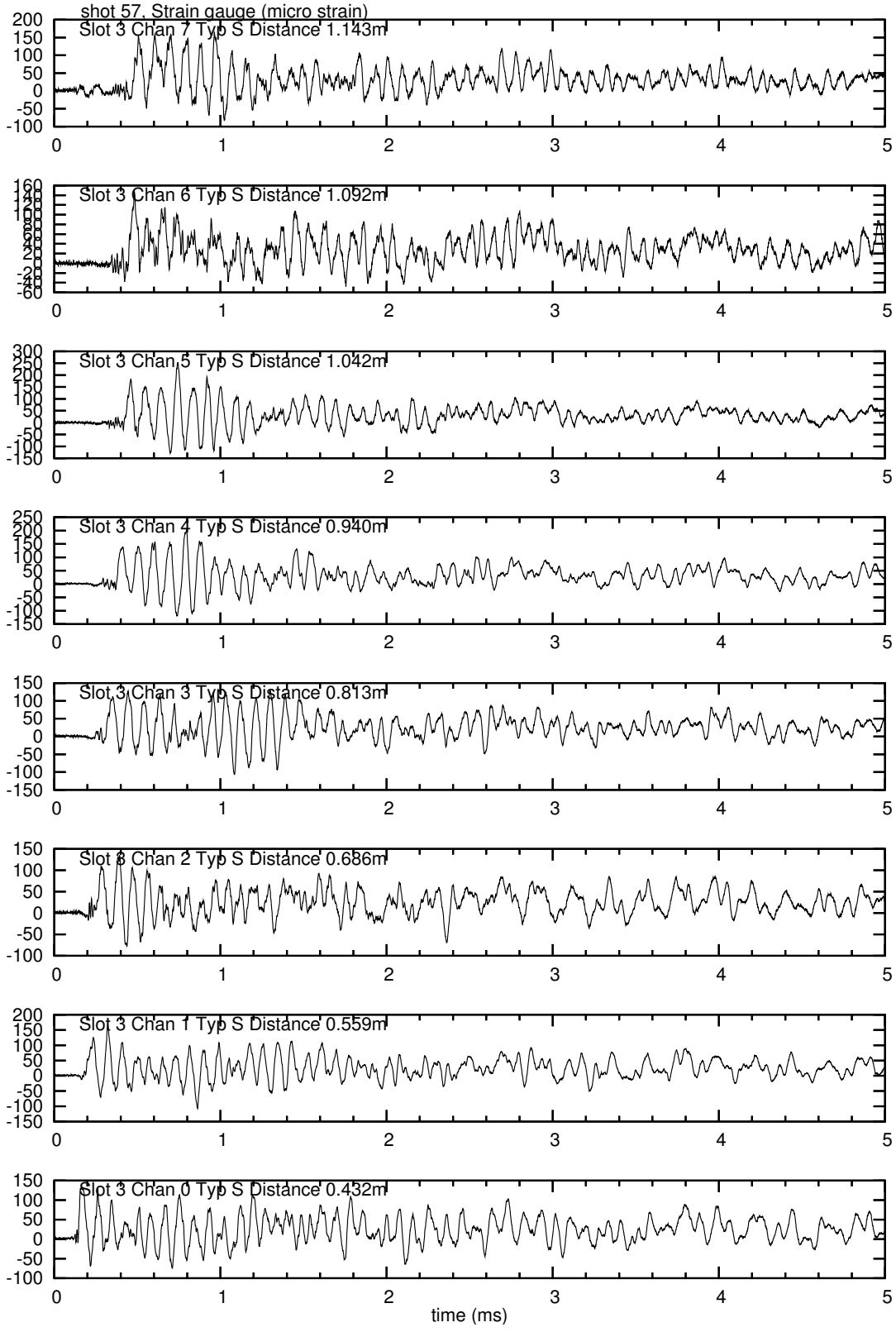

Figure 37: Strain gauges, shot 57, 30% H_2, test series B, with obstacles.

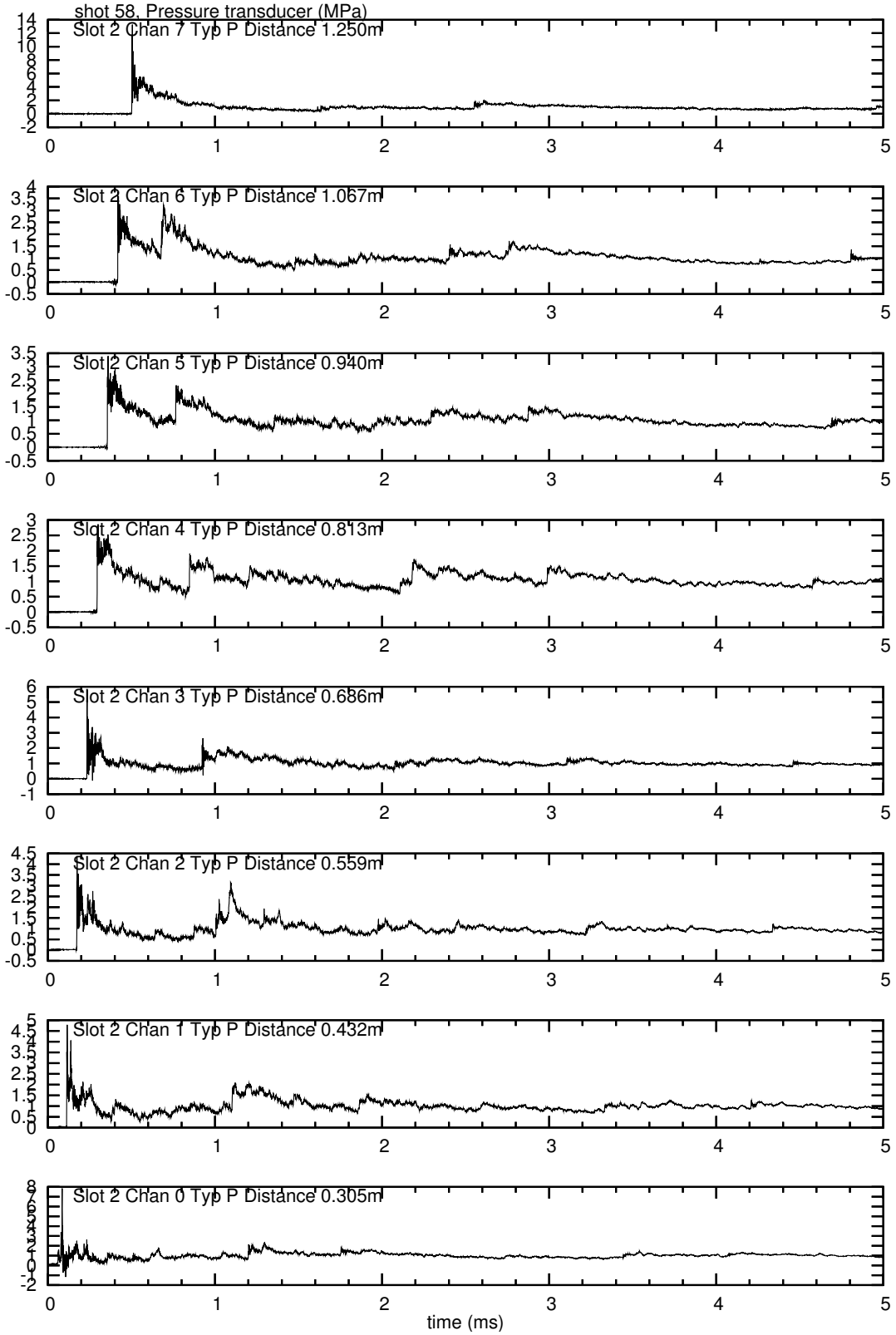

Figure 38: Pressure transducers, shot 58, 30% H_2, test series B, with obstacles.

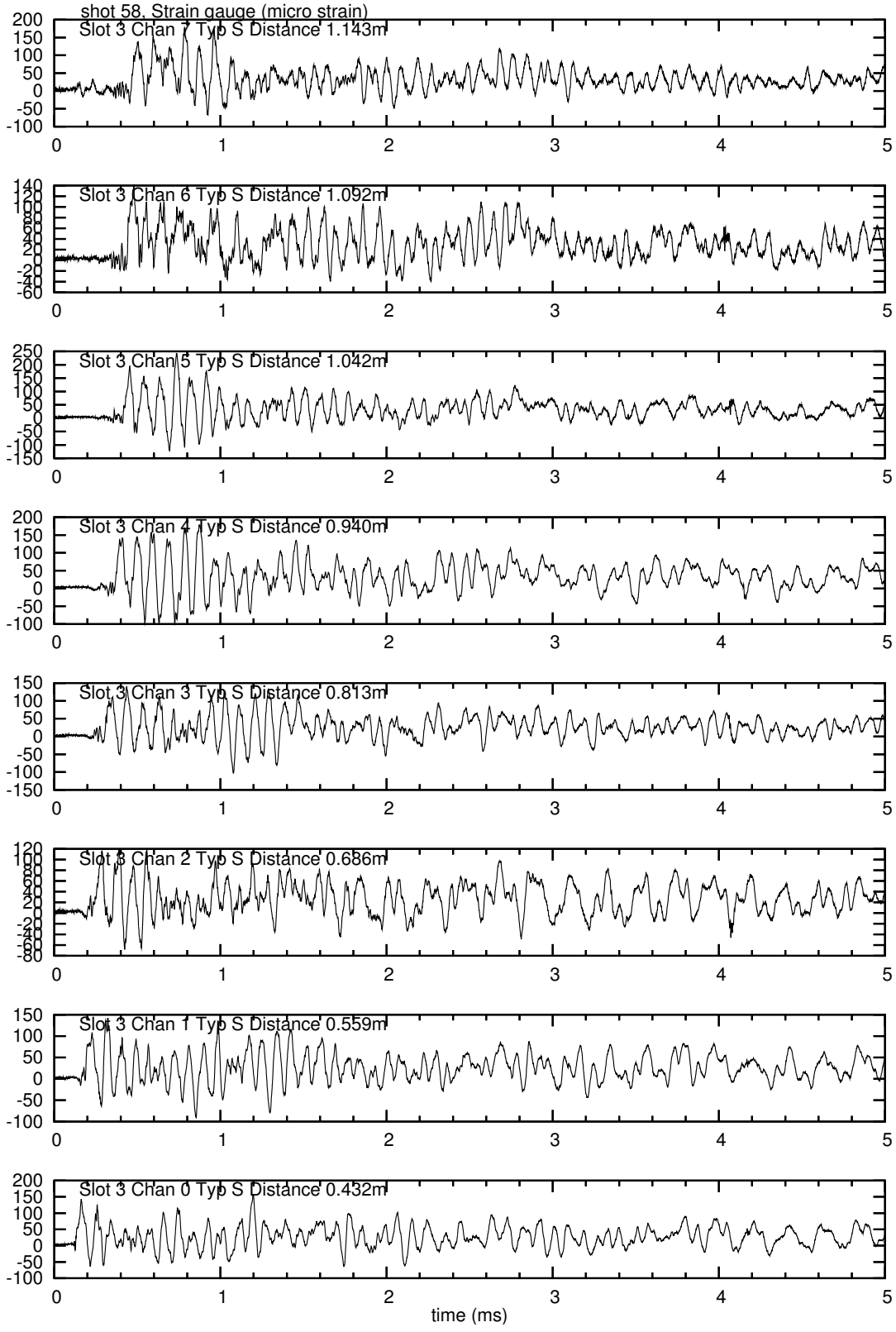

Figure 39: Strain gauges, shot 58, 30% H_2, test series B, with obstacles.